# POLITECNICO DI TORINO

Master's Degree in Electronics Engineering


Politecnico
di Torino

Master's Degree Thesis

# Development of an Optical Fiber Applicator for Interstitial Photodynamic Therapy in Minimally Invasive Cancer Treatments


Supervisors

Prof. Guido PERRONE

Eng. Aurora BELLONE

Candidate

Samuele PICATTO


October 2024

**Abstract**

Photodynamic therapy (PDT) is a minimally invasive medical treatment that exploits the activation of a drug – the photosensitizer (PS) – by light, usually from a laser. The PS is toxic to the target tissue only when activated by light. Although the elective application of PDT is the killing of malignant cancer cells, it can also be used in the treatment of many other pathologies, such as macular degeneration and skin diseases.

Important advancements in PDT have been made possible by recent studies of new PS, which have improved their light absorption and cytotoxicity effect when activated, while simultaneously reducing the side effects. However, activation light delivery remains a primarily problem in PDT, especially in the so-called interstitial PDT in which light must be delivered within deeply seated tumors without damaging other tissues. The PS can be optimized in terms of absorption and required power density, but to improve the aspects related to light delivery a suitable tool is necessary. Optical fibers can constitute an effective solution because they can be inserted in the human body through natural apertures or through thin needles, exploiting their small dimension combined with high flexibility, good mechanical resistance and all-dielectric composition.

The aim of this master's thesis is the development of a fiber optic light diffuser that can be then combined with fiber Bragg gratings for sensing the induced temperature and obtain a smart applicator for interstitial photodynamic therapy.

Effective interstitial PDT treatments require a uniform diffusion of light in the entire tumor mass. In turn, this implies that light must be irradiated not only from the tip of the delivery fiber but also from the side walls, dissipating the optical power gradually along the fiber length and isotropically around the fiber. This can be obtained by mechanical processing of the fiber, with the downside of weakening the fiber and affecting the fiber strength to bending and stress. Therefore, in this thesis an alternative approach based on the selective modification of the fiber refractive index through a femto-second laser has been studied.

The uniformity characterization of the fabricated diffusers has been performed by measuring the emissions in a phantom made of ink-loaded agar gel designed to mimic the behavior of biological tissue. The laser delivery diffuser has been placed in the center of the gel block and the uniformity of the light distribution evaluated at 3 mm from the fiber along two perpendicular axes, with four optical fiber temperature sensors based on arrays of fiber Bragg gratings (FBG-array). The light emitted by the diffuser is absorbed by the black agar that heats up, while the FBG arrays monitor the temperature change in the agar block. Reading the results collected by the sensors and relating them to the position of the arrays, it

is possible to create a 3D map of the temperature in the agar block and analyze its changes in real time. The uniformity is achieved when all the FBG-based sensors indicate the same temperature across the whole volume at every time instant.
These preliminary results show good uniformity and isotropy of the light emission, opening the possibility for extending the same fabrication method to more suitable fibers in medical applications. The results are also promising to develop future upgrades of the diffuser, such as an FBG temperature sensor addition in a smart and integrated applicator for simultaneous therapeutic and monitoring purpose.

# Table of Contents

# List of Tables

# List of Figures

# Chapter 1

# Introduction

The possibility of using light in treating illness was already known by the ancient Greeks and Egyptians, that used sunlight as a therapy. However, only with the discovery of the laser radiation a giant step forward occurred. Indeed, lasers have been found very useful in medicine, especially in surgery, often resulting to be more effective than conventional treatments with many advantages that include less blood loss, more accurate removal of unwanted tissue, shorter operating time, and less postoperative pain. For example, lasers are now widely used in dermatology and ophthalmology. Lasers (and other optical sources such as SLED) are now finding many other applications, not limited to surgery: for example, the NIRS used in diagnostics or the Photo-Dynamic Therapy (PDT) which is exploited both in tumor therapies and for antimicrobial applications. PDT involves the use of a photoactive compound, called Photo-Sensitizer (PS), which is activated by exposure to light of a specific wavelength in the presence of oxygen. Upon absorption the PS goes into an excited state in which it reacts with molecular oxygen of the living tissues and forms Reactive Oxygen Species (ROS), particularly singlet oxygen and other free radicals. ROS are very toxic to the cells as they instantly oxidize important biomolecules such as proteins and nucleic acids (DNA, RNA), leading to the dysfunction of the cells and eventually to the cell death. PDT is an appealing alternative to chemotherapy for some cancers and is exploited also in light-based antimicrobial therapies (e.g., in oral lesions). In cancer treatments, PS molecules that absorb in the Near Infrared (NIR) are desired as these wavelengths have better penetration efficiency into deep tissues than visible light.
The core research about PDT application and advancements is mainly about the development of new photosensitizers with improved features, such as better localization of the tumor and binding specificity, besides reducing the side-effects caused to the patients and improving the quantum yield of the drug, that means generating more ROS with the same irradiation power. Another aspects that is fundamental in PDT is the light delivery towards the tissue under treatment, that

should precisely drive the radiation to hit only the tumoral cells, leaving the healthy tissues untouched.
Thanks to their capacity of confining light while introducing very low losses, optical fibers perfectly suite this role, and being very flexible and resistant they are also a primary choice while dealing with medical applications. Moreover, optical fibers are completely made of silica, a dielectric material that does not interfere with magnetic radiation and is compatible with other therapies, such as magnetic resonance imaging. However, the best characteristic of optical fibers relies on their small dimensions, configuring their PDT application as a non-surgical and minimally invasive procedure, avoiding many of the drawbacks and side effects caused by surgery.
The ongoing research about delivery devices is mainly about optical diffuser, a particular device that is able to scatter light out of the fiber and irradiate it towards the external in the most uniform way, guaranteeing a uniform treatment in the irradiated region with the most predictable results. The state of the art of the diffusing devices relies on the generation of scattering using a mechanical modification of the fiber structure, such as substituting the fiber's coating with a scattering polymer, or the manufacturing of the fiber through suitable machines, such as the localized refractive index modification in the core of the fiber created by the a femto-second laser machine. The first method has the consequence of lowering the mechanical stability of the fiber, risking possible ruptures during its use in medical treatments, while the second still requires to find standard homogeneously emitting structures that can be inscribed in the fiber.
The aim of this Master's Thesis project is the production and the experimental analysis of the irradiation profile of femto-second laser inscribed diffusers, understanding whether the parameters available modify the final result and which structures are the most effective in creating a uniform emission around the optical fiber. The thesis starts with a general explanation of the principle behind lasers, optical fibers and fiber-based sensors, followed by an overview on PDT that starts with the most important information about the detailed photo-chemical reaction, to then present a general scheme of the main requirements of the therapy. In the following, there is an overview about the diffusers' working principle and their state of the art. The second part is devoted to the experimental study of the fabricated diffusers and the set up used for their characterization.

# Chapter 2

# Optical fibers, lasers, and fiber Bragg gratings

In the 1960s the advent of optical fibers completely revolutionized the world of telecommunications thanks to their long-distance and high data-rate transport. With the advancement of technology and the consequent drop of the production cost, optical fibers networks are now the most efficient and economic way to implement both long distance and short/medium range communication.
The huge importance of this communication method should not be ascribed just to fibers themselves, but the overall system must include an high-rate modulation block that generates the information then carried away by the fibers. This device is nowadays implemented through lasers, that are able to emit signals in the order of Gigabits per second thanks suitable modulation techniques not feasible for different types of light sources (such as leds).
This chapter will treat the basic principles behind optical fibers and lasers, with an overview on their possible applications not only in the communication field, but rather on the functionalization and sensing applications acquired through suitable manufacturing processes, such as Femto-second laser production of fiber Bragg gratings (FBG).

## 2.1 Optical Fibers

Optical fibers are cylindrical dielectric light guides made of glass or plastic. The basic structure of an optical fibers includes the core and the cladding, that are respectively the inner and outer part of the fiber. These two elements differentiate in having two slightly different refractive indexes and this characteristic gives the light-guiding property to fibers, thanks to the total internal reflection that takes place at the core-cladding interface. The refractive index difference between core

and cladding is in the order of 1%, obtained slightly doping the silica during the fiber production.

**Total internal reflection** (TIR) is the phenomenon in which waves arriving at the interface from one medium to another are not refracted into the second medium, but completely reflected back into the first medium. This phenomenon derives from the Snell's law:

$$n_i sin(\theta_i) = n_r sin(\theta_r)$$

that describes the relation between the angles of incident and refracted rays, named $\theta_i$ and $\theta_r$ respectively, depending on the refractive indexes of the internal ($n_i$) and external media ($n_r$), as shown in figure 2.1.

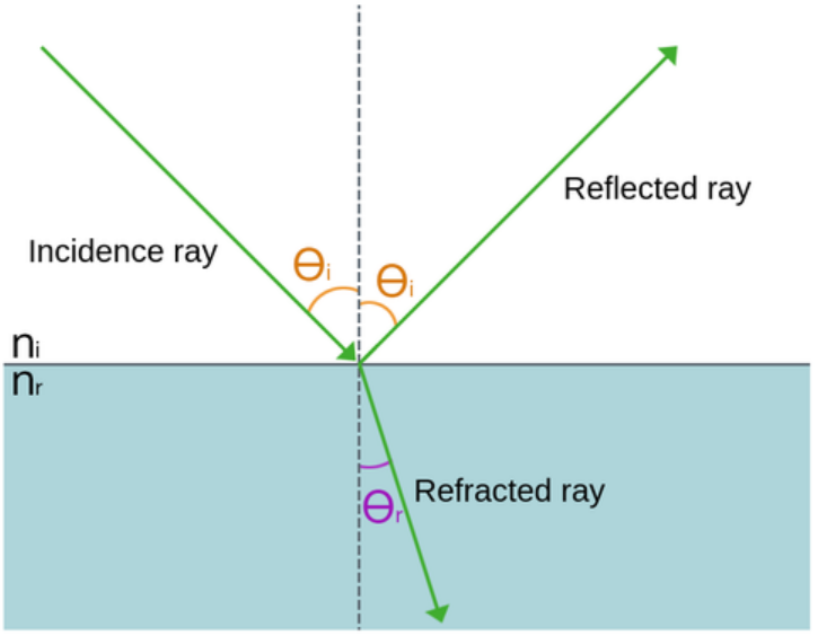


**Figure 2.1:** Graphical representation of the Snell's law.

It is also possible to define the critical angle as

$$\theta_c = arcsin(n_r/n_i)$$

that is the angle for which the angle of the refracted ray is at 90°, so that it travels parallel to the two media's interface. For incident angles wider than the critical angle, light is partially transmitted to the "external" medium and reflected back in the "internal" medium. Instead, for angles lower than $\theta_c$, the light ray is completely reflected back in the "internal" medium. It is possible to point out that TIR happens when $\theta_r$ is greater than 90°, that is when condition that can only happen when $n_r$ is lower than $n_i$.

This explains why it is important to have the refractive index difference between core and cladding, realizing the condition for light travel inside the fiber core, condition depicted in figure 2.2. The sine of the maximum angle for which the TIR condition is satisfied in the fiber core is called "numerical aperture" (NA) and is defined as:

$$NA = \sqrt{n_{core}^2 - n_{clad}^2}$$

and indicates how easy it is to couple light into the fiber core. It indicates also the the maximum angle of the output light, leading to an evaluation of the dimension of the output light spot size.

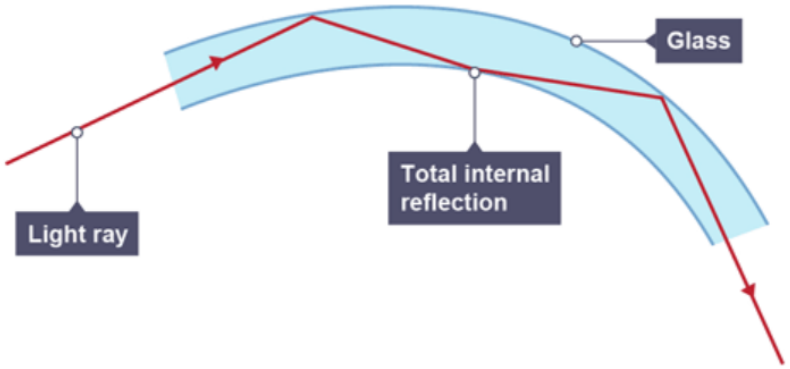


**Figure 2.2:** Example of total internal reflection.

Total internal reflection would take place even without the cladding, because the reflection condition would be valid at the interface through the glass core and air, guiding light as intended. The problem originates when the fiber touches a different material that is not just air, with a variable refractive index, not ensuring the total internal reflection condition and so resulting in leakages. The presence of a glass cladding is then fundamental to ensure a low loss condition in the fiber and to enhance the mechanical stability.

### 2.1.1 Structure of an optical fiber

The complete structure of an optical fiber should include more polymeric layer to ensure the bending and stretching properties of the final product without damaging the core, so that the fiber results to be more resistant and reliable for many types

of application. For harsh environments, an armored cable can be included. The total dimension of a fiber is in general in the order of 1 mm in diameter, while the basic core-cladding structure has a diameter of 125-140 µm. Figure 2.3 shows the alternation of layers that compose the optical fiber, starting with the core-cladding structure surrounded by a soft polymeric coating and a "stiffer" buffer to prevent any kind of puncture or damages caused by the fiber bending. The two most external layers provide an increased resistance and protection, with the Aramid Yarn being resistant to mechanical stress and flames.

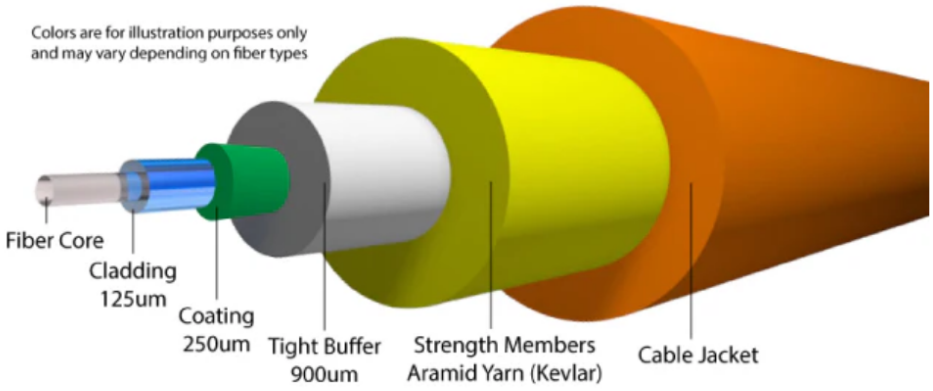


**Figure 2.3:** Optical fiber coating layers with the corresponding thickness.

The characteristics of fiber core are plenty and can be adapted to create new types of fiber, with different light propagating characteristics.
Starting from the **dimensions**, the diameter of the core can vary in a range of tens of µm but two common dimensions are 9 µm and 62.5 µm, that are respectively the standard for single-mode and multi-mode fibers. In figure 2.4 are pictured the different dimensions of the fiber core, including a different 50 µm core fiber. It is important to note that the cladding has a fixed diameter of 125 µm, hence the only dimension changing is the core size.
A mode is defined as the solution of the Maxwell equation with transversal profile and non-variable in the propagation direction. The different modes are described by different propagation constants and different modal distributions, that define their characteristics such as propagation speed, energy distribution and loss factors. An important consequence of the presence of different modes is the **modal dispersion**, originated by the different modal propagation velocities, generating a signal spread in time. The signal shape is then distorted, generating a reduction of the signal bandwidth. In a single mode fiber instead, the modal dispersion is not present and the signal can travel further thanks to the lower losses present and with larger

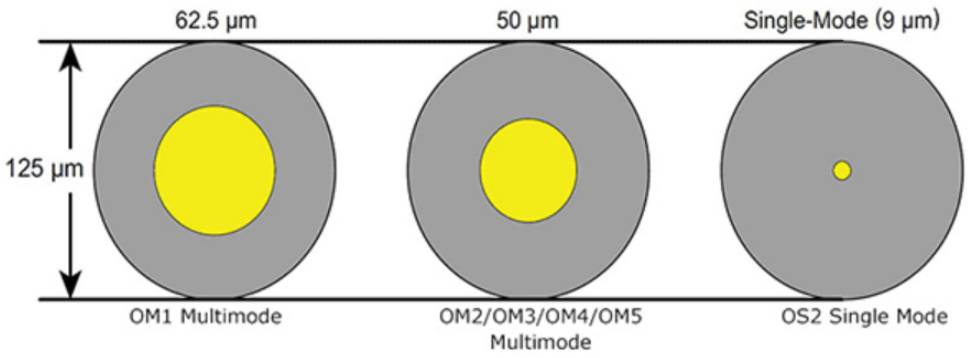


**Figure 2.4:** Examples of fibers with different core sizes used in telecommunication field. OS2 and OM1-OM5 are different kind of fibers with different cable length and data transmission rate.

bandwidth.
Another important factor regarding the core is the **shape**, ranging from the classic circular shape to elliptical or even squared shapes. The shape of the fiber is adapted to influence the **polarization** of the modes, creating polarization maintaining fibers. Finally, the **number** of cores present in a fiber can change, having multiple cores surrounded by a single cladding. The different cores can have different centers or be concentric, generating the so called **double-cladding** fibers.

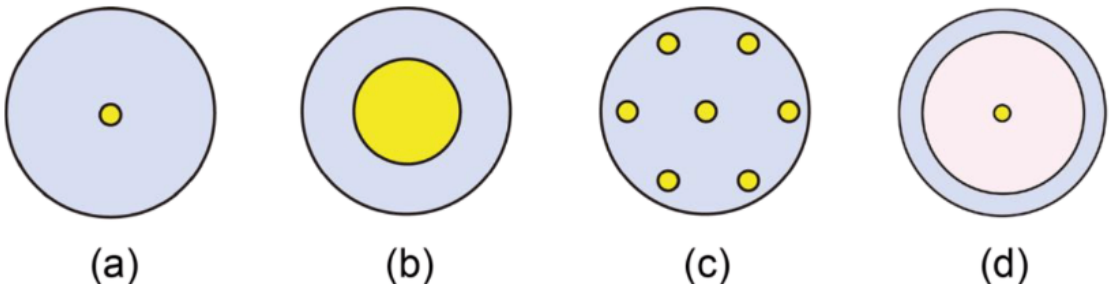


**Figure 2.5:** Examples of different fibers and core structures. a) Single mode fiber b) Multi mode fiber c) Multi-core fiber d) Double-cladding fiber.

### 2.1.2 Loss and attenuation phenomena in optical fibers

An important aspect regarding optical fibers and transmission lines in general is the reduction of losses along the whole line in order to provide a clean signal at the end of the line avoiding energy dissipation and information loss. In the case of

optical fibers there are some aspects that provide significant loss contributions and should be suppressed, where possible.
The attenuation of a fiber can be obtained as the product of the length of the fiber (L) and the loss per unit length($\alpha_{dB}$), provided in dB/km:

$$\alpha_{dB} \cdot L = (-)10log_{10}(P_{OUT}/P_{IN})$$

that is also the power difference between output and input calculated in dB.
Fiber losses derive from basically two phenomena that are material attenuation and scattering.
**Material attenuation** is given by the interaction of the light travelling through the fiber and the silica atoms, with the stimulation of electron transitions in the UV, the interaction with molecular vibrations in the infrared and the interaction with the amorphous nature of the fused silica. Moreover, there is a high absorption peak around 1383 nm due to the presence of $OH^-$ ions, that strongly interact with infrared light.

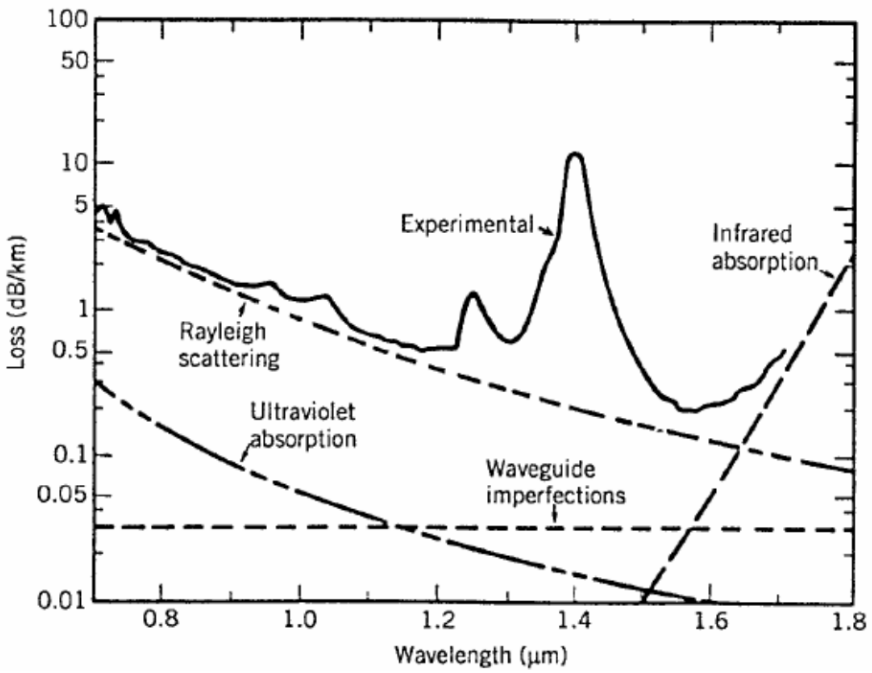


**Figure 2.6:** Total attenuation diagram of an optical fiber, representing the single components too.

Regarding the **scattering**, there are multiple factors that contribute to the total effect. In the micro-scale domain the intrinsic loss phenomena have been studied,

among which the dominant component is the Rayleigh scattering, that derives from the elastic interaction between light and particles smaller than the pulse wavelength. Elastic interaction means that the incident and scattered component have the same wavelength $\lambda$ since there is no energy loss in the photon-material interaction. The Rayleigh scattering generates a minimum loss of 0.14 dB/km and is unavoidable: a possibility is to reduce the other contributions to bring the total loss down to this limit. Currently, a single mode fiber can be fabricated to have a 0.18-0.20 dB/km loss. Rayleigh scattering is strongly dependent on $\lambda$ of the radiation, in particular the attenuation coefficient depends on $\sim 1/\lambda^4$. Another kind of elastic scattering is the Mie scattering, that derives from the interaction between photons and large inhomogeneities, with dimension comparable to $\lambda$. It derives from material or waveguide imperfections. It is less $\lambda$-dependent with respect to Rayleigh scattering, affecting uniformly all the spectrum.
Opposed to elastic and linear interaction, the inelastic phenomena cause a wavelength shift between incident and scattered light. Raman scattering derives from the interaction of an incident photon with a phonon, as are called molecular vibrations, present in the material. The particular type of phonons that take part in the Raman interaction are called "optical" phonons. Another phenomenon that has inelastic properties is the Brillouin scattering, that is the analogous of the Raman scattering but the interaction happens between a photon and and "acoustic" phonon, defined as material density fluctuations generated by thermally induced lattice vibrations. The inelastic interaction can produce an up-shift or a down-shift of the incident $\lambda$, generating respectively the so called Stokes and anti-Stokes components. In figure 2.7 is presented a graphical representation of the main scattering phenomena. The figure shows also the peaks behaviour under temperature change, that basically derives from an energy difference in the phonons due to an increased thermal stress of the lattice.
Is it interesting to point out the order of magnitude of the peak $\lambda$ variation produced by the scattering, that for Brillouin scattering is around 11 GHz, while for Raman scattering is in the order of 15 THz. Is it also possible to observe scattering-induced peak broadening, with a width difference of $\sim$6 THz for Raman scattering and $\sim$10 MHz in Brillouin scattering.

## 2.2 Lasers

### 2.2.1 Stimulated emission

A laser is an opto-electronic device that emits coherent light. Laser is actually an acronym that stands for "Light Amplification by Stimulated Emission of Radiation", a definition that briefly explains its working principle: the incoming radiation passes through a particular material, called active medium, and in the process

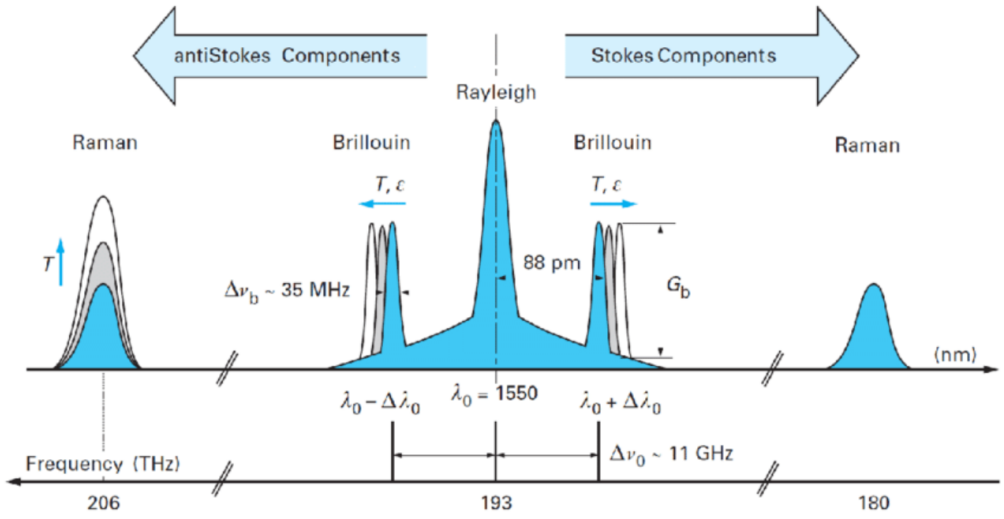


**Figure 2.7:** Diagram of the main scattering phenomena: Rayleigh, Raman and Brillouin. The diagram also shows the dependency of the $\lambda$ peaks with respect to temperature changes.

the stimulated emission phenomenon takes place, amplifying the radiation. In order to understand what stimulated emission is, we should treat it alongside the spontaneous emission and absorption phenomena, graphically depicted in figure 2.8:

- **Absorption**: happens when an electron placed on the lower level of a two energy levels system is excited through an incoming radiation (i.e. photon) and jumps to the higher energy level, but only if the photon's energy is great enough;

- **Spontaneous emission**: this is the opposite of the absorption, with an electron starting on the high energy level decays to the low energy one, emitting a photon with energy equal to the energy gap separating the two energy levels;

- **Stimulated emission**: happens when an electron already on the high energy state interacts with an incoming electron and falls to the low energy level. In this case two coherent photons with the same energy are re-emitted, generating the amplification of the incoming radiation.

  The stimulated emission is the basic physics principle of the laser emission and explains its peculiar characteristics, such as the very sharp wavelength emission range and the properties of the emitted light. The wavelength emitted by the laser is ideally just one, since the wavelength of the emitted photons derive

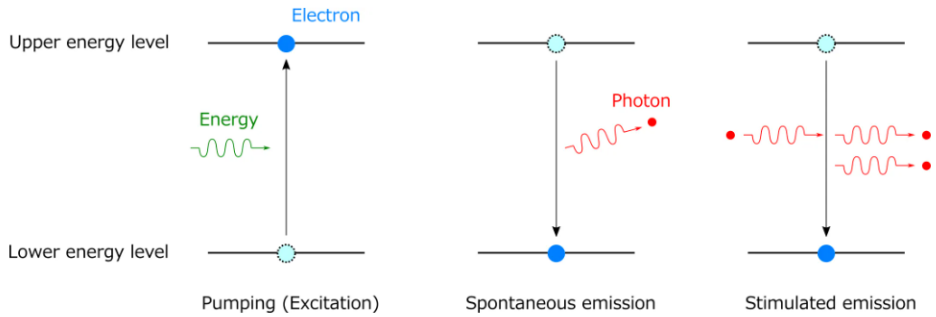


**Figure 2.8:** Spontaneous and stimulated emission.

from the energy gap that separates the two levels through the relation E=h$\nu$. The ideal case can be corrected considering that the energy levels are actually many levels close in energy, called "energy bands", in which the electron can place, generating slightly different emission wavelengths at every interaction. Moreover, the interaction with the spontaneous emission radiation broadens the emission spectrum.

### 2.2.2 Pumping

To reach the stimulated emission, the electron should be already in the high energy state, a configuration that normally is not the equilibrium state due to the residual energy present in the system. In a picture with many electrons this condition is reached when the majority of the electrons are placed on the top level, and is called population inversion. Therefore, to reach this said condition, a pumping system is needed to excite the electrons to the high energy level, and it can be done in different ways based on the kind of laser implemented. Electrical pumping is performed through a current injection that brings high energy electrons that occupy the top energy level. This kind of working principle is proper of laser diodes and solid state lasers. On the other side, optical pumping consists in generating the population inversion exciting the electrons with an electromagnetic radiation and photon of suitable wavelength and energy. This happens in fiber lasers, where the pumping and emission wavelength are different and depend on the energy gap that the electrons cover when is excited or relaxes.

### 2.2.3 Active medium

The population inversion condition cannot be reached in any kind of material and for any energy level system. The suitable materials are called "active media", a name that clearly refers to their capability of being "active", and amplify the input radiation. The simplest active medium can be modeled as in fig. 2.8, with just two energy levels separated by a fixed energy gap. In reality, this system cannot provide any laser emission since stimulated emission and pumping have an opposite effect on the system and the population inversion is never reached. Instead, a laser device can be implemented with at least a three-level system, providing an additional level moves the equilibrium of the system towards a state where the "high level" is, on average, more populated, keeping the "low level" more empty. Another possibility is the four-level system, where this process is even more favoured.
An active medium is always a single material, but rather a mixture of different elements whose energy levels combine and interact forming the multi-levels band diagram explained before. Some examples of active media can be found in ruby, Nd:YAG, glass with rare earth doping (Er, Yt), gas (He-Ne, nitrides), semiconductors (InGaAs) and many others.
In figure 2.9 is depicted a four levels energy system and its characteristics. In particular, there are some requirements to be met in order to provide an effective laser emission that depend on the time the electrons spend in the energy levels. The ultimate goal is to provide a two level system in which the high level is full of electrons, while the low level is empty: these two levels are labeled as 2 and 1 in fig. 2.9. The other two levels are the ones that provide charges to the high level and remove electrons from the low level, and are respectively labeled as 3 and 0. The peculiarity of these is the fact that the energy transitions 3-2 and 1-0 are very fast with respect to the transition 1-2, implying that the level 2 acts as reservoir for the charges coming from the pumping mechanism and from the 3-2 transition, while the level 0 acts as a charge sink, emptying level 1 and creating the population inversion condition where level 2 is much more populated than level 1.

### 2.2.4 General scheme

Now that the basic laser's amplification process have been explained, a generic laser system can be implemented to show its actual behaviour. A laser is defined as an electromagnetic oscillator which combines light amplification with feedback, where the feedback is needed to generate the stimulated emission and increase the laser efficiency. The feedback system is used to bring a portion of the output photons back to the active medium, providing the new input

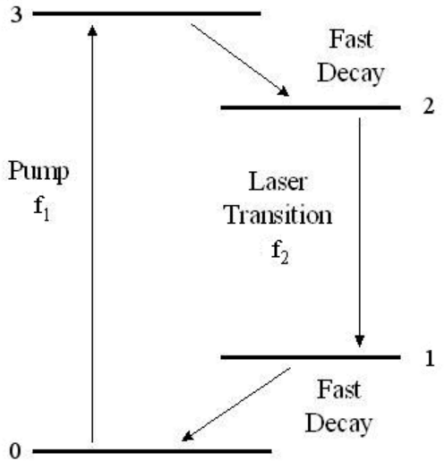


**Figure 2.9:** Four-levels energy system.

photons that will be amplified through the stimulated emission, as explained in section 2.2.1.
The feedback loop is ultimately needed to provide a gain to the amplification process so that the losses present in the laser system are compensated. If this is the case, it meas that the system satisfies the so called gain round trip condition.
There are many ways to implement the feedback mechanism that basically depend on the type of laser implemented. In the case of laser diodes the active medium is a waveguide (i.e. structure that confines and guides light) confined between two refracting mirrors, one with a high reflectivity and the other with a lower one. The Feedback is given by the reflection happening between these two mirrors that sends back and forth the photons, keeping the stimulated emission active. The output of the laser is given by the low reflectivity mirror, also called output coupler, that lets a small part of the photons to exit the cavity: this contribution, plus the eventual losses intrinsic to the cavity, are the ones that the gain of the feedback loop has to compensate.
This feedback structure is called Fabry-Perot cavity, and the mirrors/reflections can be implemented in different ways, such as trough Bragg reflectors or distributed feedback.
Another possibility regards the fiber lasers, in which the feedback system is analogous to the Fabry-Perot cavity but integrated in the fiber. The fibers used to implement a fiber laser are called active fibers, that are similar to the normal ones but doped with rare earth ions, constituting the active medium of the laser. The two mirrors of the cavity have the same reflectivity criteria explained before, but now they are integrated inside the fiber through the

creation of the so called fiber Bragg Gratings, a particular structure generated by the periodic refractive index change of the glass that acts as a sharp wavelength filter.

### 2.2.5 The role of spontaneous emission

The picture proposed explains how the laser works and the principle of feedback associated to the stimulated emission, but the turn on procedure to generate the amplification is yet to be explained. The stimulated emission is generated when the electrons in population inversion are interact with a photon, but at the beginning the stimulated emission is not present and the feedback does not provide any photon to start the lasing mechanism.
The solution comes from the spontaneous emission of photons, that naturally occurs during the population inversion due to the multitude of electrons present on the high energy level which decay spontaneously to the low energy level. This process generated a photon for every decayed electron, generating what will be input photons of the stimulated emission.
It is important to highlight that the number of photons generated through stimulated emission is much higher than the photons generated via spontaneous emission, resulting in the laser emission composed almost entirely by stimulated photons. Still, the spontaneous emission is present even if in terms of power it is practically imperceptible, but generates an interesting side effect: the spontaneous emission noise. This noise is one of the causes for which the laser output is not exactly a single wavelength, as the quantum theory would suggest, but is rather a sharp interval of wavelengths generated by the spontaneous emission.

## 2.3 Fiber Bragg Gratings

The fiber Bragg grating (FBG) is an in-fiber element made by a periodic variation in the core refractive index, which generates a wavelength-specific dielectric mirror. The selected wavelength, called Bragg wavelength $\lambda_B$, depends on the grating period through the relation

$$\lambda_B = 2n_{eff}\Lambda$$

where $n_{eff}$ is the effective refractive index of the core while $\Lambda$ is the grating period.
Fiber Bragg gratings are important components in fiber manufacturing for

their filtering capability and to implement optical sensors for strain and temperature. This comes from the fact that the Bragg wavelength depends on these two physical quantities, generating a wavelength shift that can be measured and related to the corresponding quantity. The dependency of $\lambda_B$ on temperature and strain happens due to the dependency of $n_{eff}$ and $\Lambda$ on these said quantities, since both tend to modify the physical structure of the grating via temperature expansion and mechanical pulling of the fiber, that ultimately lead to a modification of the physical periodicity of the grating and the internal structure of glass, implying a refractive index change. Typical values of wavelength shift for these kind of sensors can be 1 pm/$\mu\epsilon$ for the strain sensitivity and 10 pm/°C for the temperature sensitivity. Figure 2.10 shows the behaviour of an FBG, with an input broadband signal that passes trough the fiber almost entirely, losing just the signal portion at the Bragg wavelength that is reflected back.

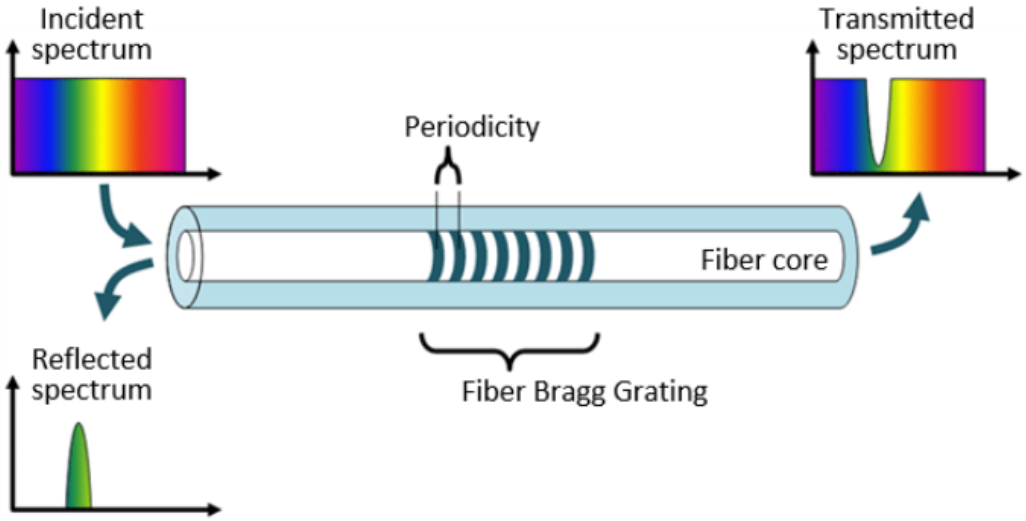


**Figure 2.10:** FBG working principle. A broadband signal travels inside the fiber, meets the FBG and just the component at the Bragg wavelength is reflected, while the others remain unperturbed.

The complete dependency of the Bragg wavelength on temperature T and

strain $\epsilon$ can be derived as follows:

$$d\lambda_B = \left[\frac{\delta}{\delta\epsilon} 2n_{eff}\Lambda\right] d\epsilon + \left[\frac{\delta}{\delta T} 2n_{eff}\Lambda\right] dT$$

and concludes in

$$d\lambda_B = \left[2n_{eff}\frac{\delta\Lambda}{\delta\epsilon} + 2\Lambda\frac{\delta n_{eff}}{\delta\epsilon}\right] d\epsilon + \left[2n_{eff}\frac{\delta\Lambda}{\delta T} + 2\Lambda\frac{\delta n_{eff}}{\delta T}\right] dT$$

The wavelength shift upon strain and temperature influence is described by the following equation, obtained dividing the preceding equation with the characteristic equation of FBGs

$$\frac{d\lambda_B}{\lambda_B} = \left[\frac{1}{\Lambda}\frac{\delta\Lambda}{\delta\epsilon} + \frac{1}{n_{eff}}\frac{\delta n_{eff}}{\delta\epsilon}\right] d\epsilon + \left[\frac{1}{\Lambda}\frac{\delta\Lambda}{\delta T} + \frac{1}{n_{eff}}\frac{\delta n_{eff}}{\delta T}\right] dT$$

The variation of temperature and strain condition induces a change in the pitch $\Lambda$ and in the refractive index $n_{eff}$ of the FBG, producing a shift in the Bragg wavelength $\lambda_B$.
In the case of a macroscopic variation, the equation becomes

$$\Delta\lambda_B = K_\epsilon \cdot \epsilon + K_T \cdot T$$

being $K_\epsilon$ the strain sensitivity and $K_T$ the temperature sensitivity, whose values have been given above.
Care should be taken when analyzing the $\lambda_B$ shifts since, if the wavelength shift depends both on temperature and strain, it is not possible to separate the two components using just a single sensor, but a differential measurement should be carried out. Equivalently, when measuring just one of the two parameters, the operator must exclude any possible influence deriving by variations of the other quantity, otherwise the result is not reliable.

### 2.3.1 FBG manufacturing

FBGs are produced "writing" the periodic structure inside the fiber core trough a UV laser light, that modifies the refractive index of the glass according to the radiation intensity. Four methods are commonly used for the manufacturing:

– Interference: this was the first method developed and exploits the properties of interference pattern to write the FBG. The laser beam is split in two paths that will recombine forming the periodic interference pattern inscribed in the fiber;

- Photomask: a physical mask suitably patterned is placed between the light source and the fiber, shadowing the regions that should not be affected. It is used for particular FBG that are not reproducible trough interference;
- Sequential writing: this method exploits the production of multiple partially overlapping gratings to create a final FBG with more complex properties;
- Point-by-point: a laser with narrow output beam is used to write directly on the fiber one point at a time.

# Chapter 3

# Photodynamic therapy

Photodynamic therapy is an emerging noninvasive treatment modality, which involves the use of a photosensitizer (PS), light and endogenous molecular oxygen to kill cancer cells or microbes. Individually each component is non-toxic, but when PS is irradiated with light, the photochemical reactions result in the formation of highly reactive singlet oxygen species that are responsible for cytotoxicity and cell death via apoptosis[1]. First discovered at the beginning of the 20th century, PDT has seen a major development after the first controlled clinical study in humans, in 1978. The therapy has evolved with the development of improved photosensitive drugs and new light delivery techniques, making PDT a valuable alternative to traditional cancer treatment also having minimal normal tissue toxicity, negligible systemic effects, greatly reduced long-term morbidity, lack of intrinsic or acquired resistance mechanisms, and excellent cosmetic as well as organ function-sparing effects [2]. The on going research about this topic is further improving the therapy, allowing an always greater number of tumors to be cured.

The principle behind PDT is the photochemical reaction that generates radical ion species (ROS) upon PS irradiation. Upon all, singlet oxygen is the ROS with the most cytotoxic effect and the main component on which the therapy relies.
In order to arrive to the final effect, the PS should be correctly delivered to the cancer region via injection or through oral administration. Once the drug has correctly reached the designed spot it should be irradiated through a suitable light, able to react with the PS. The light irradiation depends on the type of tumor under treatment, and requires different type of delivery system suitable for the situation. Finally, also the wavelength of the irradiation has an important role, because different wavelength can penetrate more under

the tissue and be more effective in reacting with the photosensitizer, without generating any side effect.

## 3.1 The photosensitizer

The role of PS is crucial for the result of PDT and the on going research is trying to create the best PS, minimizing the risks for the patient while curing the disease to the best. The most important characteristics of a photosensitizer are [3]:

- **Absorption wavelength and absorption coefficient**: these two values indicate the reactivity of the PS to light, and define the wavelength that the PS is most sensitive to;
- **Quantum yield of excited PS state and of singlet oxygen**: the quantum yield indicates the number of times a specific event occurs per photon absorbed by the system, so the number of excited PS and singlet oxygen generated per incoming photon. It should be the highest possible in order to have the most efficient photochemical conversion rate;
- **Dark toxicity**: this data is the toxicity of the PS when it has not been irradiated yet. PS should be inert when not exposed to avoid generating any unwanted reaction in healthy tissues;
- **Clearance**: the rate at which the active drug is removed from the body. The higher the clearance, the lesser the patient should be kept under control;
- **Selectivity and selective accumulation**: the capability of a PS to correctly select the target cells and localize its accumulation in that region, improving the drug delivery;
- **Solubility in biological media**: a molecule is easier to inject in the body if it is soluble and inert to the biological environment present in the body.

These characteristics are the focus of the PS research and every new generation of PS drugs aim to improve some of these aspects. In particular, there are three classes of PS named first, second and third generation PS that represent the chronological evolution of the drug and differ in their working principle, trying to improve the most critical aspects relevant for the therapy.
**First generation** PS are the first photosensitive drugs developed. In the early 1950s the observation that haematoporphyrin tend to localize in tumour tissues accelerated the research to develop a porphyrin-based PS, resulting

in the FDA approval of Photofrin for treating lung cancers, bladder cancers, esophageal cancer and early stage cervical cancer: Photofrin and haematoporphyrin are considered as first generation PS [1].
However, approved for a wide variety of cancer treatment, it has many drawbacks like lack of specificity, cutaneous phototoxicity, hydrophobicity and weak absorption in the therapeutic window[1]. Moreover, the absorption peak is localized between 400-650 nm, in the visible spectrum, where the penetration capability of light is greatly reduced and can be used just for superficial and cutaneous treatments. Another important drawback is that this kind of PS can be retained in the tissue for up to ten weeks post-injection. This causes a marked skin photosensitivity that requires the patient to avoid bright sunlight, this being an obvious disadvantage especially for patients with late-stage malignancies.[4]
To address the above issues, **second generation** PS with near infrared (IR) absorption and high singlet oxygen quantum yield where developed. As an example, AminoLevulinic Acid (ALA) has been considered as a valid PDT agent thanks to the endogenous accumulation of protoporphyrin IX following the administration (systemic or oral). FDA approved ALA to cure many diseases like cutaneous superficial and nodular basal cell carcinoma, Bowen's disease, and actinic (solar) keratoses, superficial head and neck cancer, gastrointestinal cancers[1].
**Third generation** PS have been developed to further improve drug delivery, cancer specificity and target localization, solving the weak localization capability of second generation PS. The basic idea is to conjugate the photosensitizing agent to a carrier bio-molecule or targeting agent, improving the specificity of the molecule, reducing off-target effects, and improving molecular reactivity. With the advent of modern technologies, suitable nano-particles have been studied to overcome the limitations of traditional PS, engineering the nano-carriers to many different uses.

### 3.1.1 The photochemical reaction in detail

The product of the reaction between PS and oxygen is not simply the highly reactive singlet oxygen, and another distinction has to be made. The reactions that the PS undergoes are divided in **type I** and **type II**: both derive from the excited PS that loses its energy interacting respectively with an organic molecule or with molecular oxygen. The results of these two types of reactions are $OH^-$ radicals and superoxide ions for type I and singlet oxygen for type II. The detailed process (figure 3.1) consist in the PS initially at energy ground state (S0) absorbing a photon, with an electron transferring to an higher energy orbital. This configuration is named excited singlet state (S1) and

is very unstable and short-lived, hence it cannot directly react with other molecules. Here, two thinks can happen: the PS can emit the energy excess through heat and fluorescence, or it may undergo an intersystem crossing, that is a rearrangement of the electrons spin to a more stable configuration, called triplet state PS (T1). Now, thanks to the longer lifetime, the PS can react with other molecules or decay radiationlessly to the ground state. If an interaction occurs, it can be with molecular oxygen ($^3O_2$) (type II reaction), generating singlet oxygen ($^1O_2$), or it can be with an organic molecule (type I reaction). It is believed that type II reactions are the most common, dominating the PDT mechanism. [2]

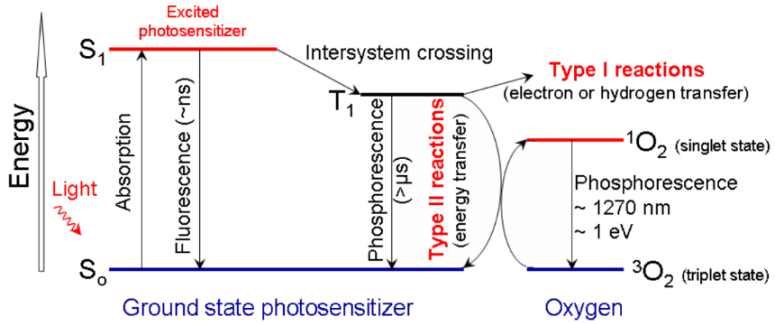


**Figure 3.1:** Energy scheme (Jablonsky diagram) of the photensitizing reactions.

A clarification has to be made about the terms singlet and triplet state. When referring to the PS, the singlet state is the stable ground state that can be excited to reach the semi-stable triplet state. The opposite is true for oxygen, where the triplet state is the stable ground state while singlet oxygen is the excited form. This difference is present since the terms singlet and triplet refer to the electrons configuration of the molecule under analysis and not to the total energy of the system, as shown in figure 3.2.
Generally, a molecule in its singlet state is also at its ground state, since the two electrons on the highest orbital have opposite spin guaranteeing the lowest energy and most stable configuration. Molecular oxygen is an exception to this rule since its ground state has the electrons in the triplet configuration, described in figure 3.2, while the excited state coincides with the singlet oxygen.
Summarizing, the electronic configuration of the molecules is such that during PDT the singlet state PS absorbs the incoming photon, transitioning to the triplet state. The triplet state PS now reacts with molecular oxygen in its low energy triplet state, giving away the energy excess that excites the molecular oxygen to its highly reactive and cytotoxic singlet state.

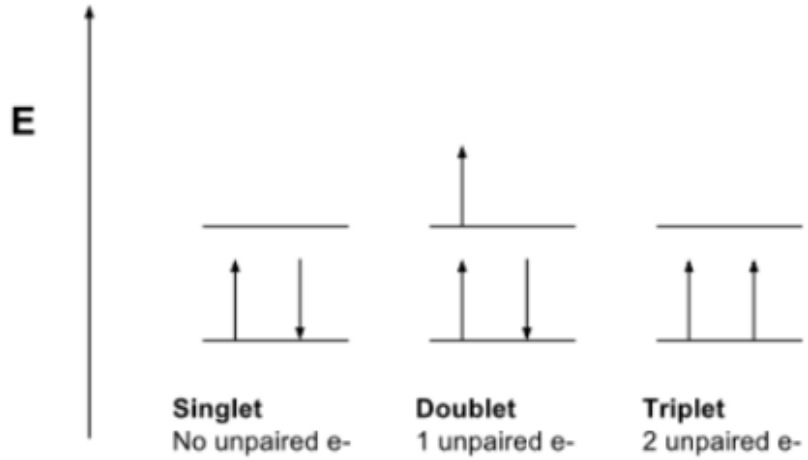


**Figure 3.2:** Energy diagram and electronic configuration of singlet, doublet and triplet state.

### 3.1.2 The nano-particles approach

An interesting evolution of PS is the development of nano-particle based PS and the advent of nanoparticle-based carriers to improve the drug delivery system. The nanomedical approach proposes the study of small molecules (1-100 nm) and nanomaterials with improved characteristics, such as drug delivery to the target area. Among other advantages, the most important are the improved solubility of poorly soluble drugs, the minimized drug degradation, the decreased side effects, the lower toxicity and the better biocompatibility.[5]
The high specificity of functionalized nano-carriers is another great asset of the nanomedical approach. Also thanks to their size, nanomaterial are capable of accumulating in the tumour areas due to the enhanced permeability and retention effect (EPR effect) of pathological areas, where the vascular system is less strong and leads to leakages in the cancer region. The pore size in tumours varies in 100-750 nm, allowing the nanoparticles flow and accumulation in the unhealthy tissues.[5]
The idea behind nano-carriers is to encapsulate the PS in a shell, that is the engineered nanoparticle, to improve its chemical properties and behaviour, conferring it enhanced solubility, stability and selectivity thanks to the addition of functional groups (e.g. antibodies).The delivery agent in which the PS in contained can be in the form of liposomes, micelles, ceramic based nanoparticles, gold nanoparticles, polymer nanoparticle.

Regarding the nano-PS, there exist nanoparticles that do act as PS themselves and generate ROS upon illumination. There are several types of particles used such as biodegradable, non-biodegradable, passive or active nanoparticles, quantum dots: these classes are not a strict classification, but differ on the basis of various characteristic that make a PS more suitable for an application respect to another. Some examples of nano-PS can be found in gold nanoparticles, carbon nanotubes, fullerenes, ZnO nanoparticle, $TiO_2$ nanoparticle and others that can be combined and engineered to obtain the desired characteristics.

### 3.1.3 Gold nanoparticles

Among the various kinds of nonoparticles listed above, gold nanoparticles have raised a considerable interest in the field, thanks to their remarkable light-to-thermal energy conversion efficiency and their property to load and deliver plenty of different anticancer drugs[6].
Gold nanoparticles are used in PDT as PS carriers, but they also have the role of thermal agent in photothermal treatments (PTT). Their effectiveness comes from the strong interaction with light, generating resonance phenomena in the particles through energy excitation. In particular, just a specific wavelength is able to excite the resonance in the form of SPR, that is the resonance of the collective oscillations (plasmon) of the surface electrons. The specific wavelength that the plasmons interact with depends on the shape, size, surface and aggregation state of the nanoparticles [6], opening the possibility for tuning the characteristics of the nanoparticles adapting their fabrication process. Moreover, the absorption wavelength is not unique since the plasmon present in a particle have different characteristic mostly dependent on the shape and size of the particle, where the number of peaks present in the absorption spectrum depends on the number of different plasmons that can be excited.
These aspects are of particular interest in PTT, where the most important result that the nanoparticles should provide is an high light-to-heat conversion factor for the incoming radiation: for gold nanoparticles in general, this factor ranges form 22% to 103% and is generally higher for nanoparticle with smaller radius, where the absorbance/scattering ratio is higher. Despite this, larger nanoparticles have shown experimentally the ability of reabsorbing the scattered light coming from other nanoparticles, increasing the total absotpion resulting upon illumination. In conclusion, the most suitable and effective nanoparticle characteristics must be chosen based on the specific application.

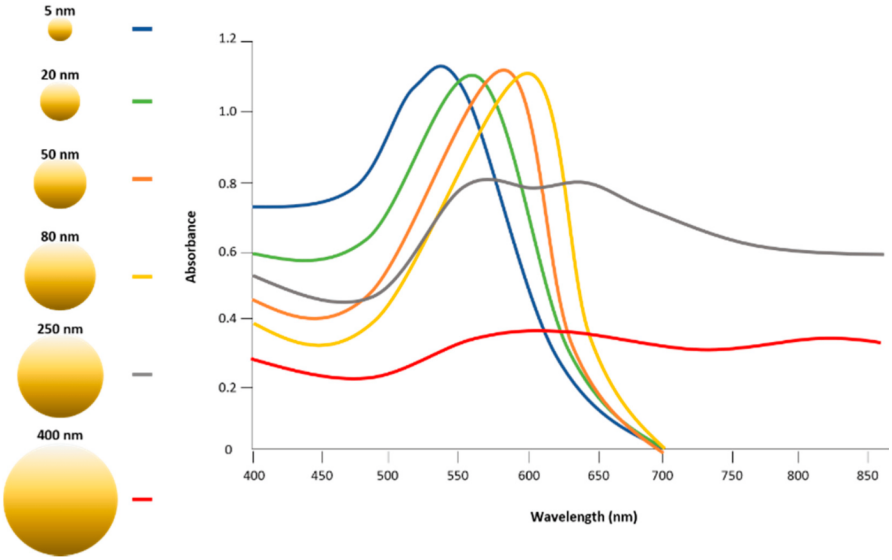


**Figure 3.3:** Gold nanoparticles absorption spectra depending on the size, highlighting the different wavelength that generate the plasmon resonance.

Regarding PDT, gold nanoparticles are used as suitable biocompatible carriers for PS, mostly in hydrophobic environments, or in alternative the PS can be conjugated on the nanoparticle surface or encapsulated in it.
The gold nanoparticles may interfere with the illumination of the PS during PDT treatment, however the PS inside of the nanoparticles is better protected from the destruction mechanism of the immune system with the respect to PS surface linked to the nanoparticle. The transport mechanism ends when the PS reaches the tumor zone and detaches from the carrier's surface, either spontaneously or enzymatically.

## 3.2 The importance of light

Light is among the most important components in PDT, having the role of delivering the energy to start the photochemical reaction. In PDT, the most characteristic of the incoming radiation are:

– Power delivered: the power should be high enough to excite the PS to its reactive state, but should not generate high temperature regions that may be dangerous for the tissues, causing heat induced apoptosis or even thermo-ablation. Usually in PDT the power used is in the order of a Watt;

– Wavelength: long wavelengths penetrate more in the tissues with respect to shorter ones, so NIR wavelength are now used in PDT. Moreover, the wavelength of the radiation should be the one that maximizes the absorption from the PS;
– Dose: it is the number of incoming photons per unit area in the unit time. Has to be correctly tuned to maximize the effect of PDT and avoid over-reactions.

These aspects should be suitably studied and depend on the kind of tumour to be treated and the PS in use. With first generation PS the light used was in the visible spectrum, ensuring high photon power but with reduced penetration capability; it has been studied that NIR wavelength can penetrate deeper in tissues thanks to longer wavelength and the reduced interaction with the chromatofores and cells present in the tissues (fig. 3.4): the region 600-1200 nm is called optical window of tissues. However, photons with more than 800 nm wavelength do not have enough energy to start the photochemical reaction. Despite this considerations, blue and UV light are commonly used for superficial treatments, such as acne and skin diseases .

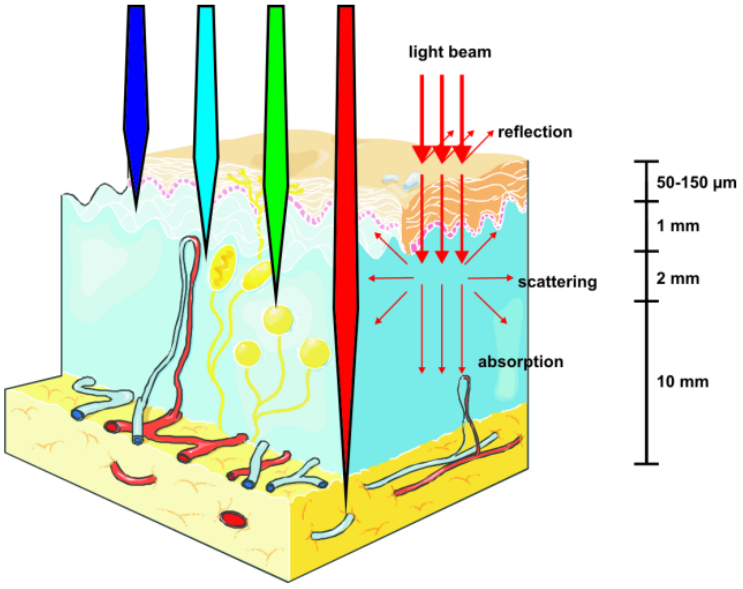


**Figure 3.4:** Light penetration depth depending on wavelength.

Regarding light dosimetry, it should be correctly tuned and measured throughout the entire procedure to keep under control the effects of the therapy. The correct dose is the one maximizing the number of reaction in the unit time

without compromising the the effectiveness of the irradiation. A possible risk of using a wrong dose is the consumption of molecular oxygen in the tissue at a rate higher than the tissue can re-oxygenate. Oxygen is the precursor of singlet oxygen and is then consumed in the reaction with the PS. If molecular oxygen has been completely transformed to singlet oxygen there is no more precursor available and the photochemical reaction stops, leading to an inefficiency in PDT. Given this, it is important to correctly balance the consumption rate and re-oxygenation rate, resulting in the highest maintainable production of singlet oxygen.

### 3.2.1 Light sources

The property of the delivered light are strictly related to the light sources that in PDT are mainly lasers, light emitting diodes (LEDs) or lamps. The choice of the light source depend on the photosensitiser, the localization of the target and the dosimetry needed, with a strict correlation to the light delivery technique implemented: optical fiber-based devices are the most suitable for minimally invasive procedures and can deliver light very close to the target.
**Lasers** are widely used for interstitial and superficial PDT, effective thanks to their coherent monochromatic output, with very narrow bandwidth. The laser emission can be tuned to correspond to the wavelength of the absorption peak of the PS, but for different PS also different laser sources may be needed to effectively produce the photochemical reaction. The high-power collimated output of lasers makes optical fiber a perfect delivery medium to carry light in the desired spot for endoscopic and interstitial application. For superficial treatments, that need to cover a larger tissue area with uniform irradiance, beam expanders can be coupled with the output of the laser. The kind of laser most used for this application are the laser diodes, but alternatively dye lasers can be employed.
**LEDs** are an available alternative to lasers with the advantage of being low-cost and portable devices. Compared to lasers, LEDs generate lower output power compared to lasers with a wider spectral width, resulting in lower compatibility with the PS absorption peak and lower efficacy of the photochemical conversion. The main application of LEDs is for treating superficial tumours, but LED arrays can be used for endoscopic treatments too. The main problem of LEDs in interstitial PDT is the heat generation deriving from a low electrical to optical conversion efficiency.
**Lamps** where the first light sources used for PDT, with their simple design, low cost and broad irradiation. The output can be coupled to light guides for localized treatments, but implies high coupling loss, making lamps more suitable for broad superficial treatments. The most important drawback of

lamps in PDT application is the broadband spectrum of the output (300-1200 nm) that needs to be filtered to correctly match the peak absorpyion wavelength of the PS. Optical filtering is also required to take away unwanted ultraviolet and IR radiation that could interfere with the treatment[7].

# Chapter 4

# Delivery devices and diffuser's state of the art

Light delivery is a crucial problem in the field of phototherapies, mainly when the treatment has to reach regions deep inside the human body with high precision. A global, all-around illumination of the patient is always possible when the procedure is carried out on the skin, but light penetration limits to the outer layers of the cutaneous tissues. In order to further evolve therapies that involve the used and delivery of light, suitable tools have been and are still developed to provide the maximum efficacy to the treatments.
Part of this problem is solved using optical fibers, that are able to guide the light generated by a laser or a led for many meters without significant power loss, delivering all the provided optical power towards the distal end of the fiber, where the treatment area is located. In medicine, the small dimensions, high flexibility and high mechanical resistance are the prime advantages provided by optical fibers, that can be applied to medical procedures performed on areas seated deep inside the human body guaranteeing the necessary safety standards for the patient. Moreover, since fiber are completely made by dielectric materials (plastic or glass), their usage is compatible with other therapies that involve electromagnetic irradiation, such as radiotherapy or magnetic resonance imaging (MRI), without causing any interference or compromising the other therapies.
The limitation of optical fibers stands in their light emission profile. Since the light is completely emitted from the tip, all the delivered power is focused in a small volume and the irradiation is confined in a localized spot with very high power density. In practical applications the region under treatment is usually much larger than a single spot, and the necessary power should be

spread all over the surface of the tumor. If the power is too concentrated, the temperature will raise to cito-toxic level, producing the effect of a PTT or thermoablation that employ an high temperature in order to kill the cancerous cells. In the case of PDT and other photo therapies, the power delivered in every point is quite low compared to PTT, because the energy is needed just to excite the PS that will then provide the chemical reactions to kill the malignant cells. However, it is necessary to uniformly and homogeneously irradiate the area under treatment in order to obtain better and more predictable results, hence the light diffusion should be done in a controlled manner.
Light diffusers are the tools suitably designed to perform this task. Differently form the light delivery system, that are selected to guide light and bring it far from its generation point, light diffusers are created to dissipate all the optical power in few centimeters, directing it to the designed target. There exist many kinds of light diffusers depending on their fabrication procedure, materials employed and emission profile, but there is not a best alternative: in PDT, depending on the size, shape and location of the tumour, a suitable diffuser should be chosen to provide the best results for the treatment. In general, thanks to the small dimensions of the probe, PDT is configured as a minimally invasive procedure.
This chapter will be an overview on the different types and manufacturing of light diffusers, explaining their evolution and possible applications and focusing on possible application in the PDT field.

## 4.1 Achieving light diffusion

Within the many kinds of diffusers available, a common ground can be found in the use of optical fibers for light delivery. Especially in minimally invasive procedures, diffusers are coupled to the output of the optical fibers regardless of the specific application, defining the geometrical and technical parameters for the design of the diffusers, such as the maximum power that the probe should withstand or the low loss connection to the fiber output.
Since the PS-activation light comes from an optical fiber, the most immediate idea to achieve light diffusion is the manufacturing of a proper fiber tip. The first experiments where done shaping the fiber tip with different geometries, obtaining a directional emission of light, not just in front of the tip but also sideways. This kind of probes are called "side-firing" which are fabricated cleaving the fiber tip at certain angle such that the total internal reflection makes the light come out of the fiber at a right angle, opposite to the front-emitting flat cleaved fibers. Another possibility for shaping the fiber tip is to melt the silica of the fiber creating a circular droplet of fused glass, that

then solidifies forming a "ball-shaped" tip, whose emission profile is mainly forward oriented but with a different energy distribution with respect to the flat cleaved tips. Shaping the fiber tip gradually reducing the diameter of the fiber's end segment originates the "tapered" tips, another common type of diffuser. Tapers are created locally heating the fiber while pulling the fiber core apart. Ball-shaped and tapered tips are used to increase the optical density in front of the tip, and are used to deliver high powers in a localized spot.
A different alternative is presented by placing microlenses or a sphere of scattering material in front of the tip, creating either a focusing or isotropic irradiating probe. Also, a metal tip can be added to convert the optical power in heat. In order to protect the tip of the fiber and prevent any interference from the external environment on the optical effect, such as in aqueous media, the fiber tips are covered and protected with an optical shield. The fiber end can be either placed on the surface or inside the tumor through a catheter or endoscope, allowing the internal illumination of the tissue or organ.[8]
Some examples of the listed fiber tips are presented in figure 4.1.

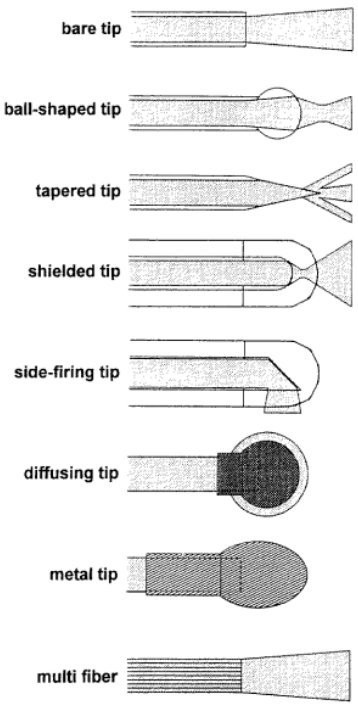


**Figure 4.1:** Examples of modified fiber tips with different emission profiles.

These listed types of diffusers imply the front coupling with light. Alternatively,

diffusers could be designed to implement the principle of radial coupling, that is the diffusion of light from the sides of the fiber instead of the front, creating a cylindrical diffuser. This kind of fibers can be developed in different ways, starting with a mechanical modification of the fiber by removing the buffer and cladding layers and substituting them with a polymeric layer doped with highly scattering material, such as $TiO_2$ [9]. The cross section of the result is shown in figure 4.2.
This fabrication procedure has a critical drawback, since it requires to leave the core unprotected for some time, making the fiber extremely fragile. The polymer coating applied does not solve this issue since it is rather rigid and easy to brake. This aspect is critical in medical procedure, rendering a possible interstitial therapy dangerous.

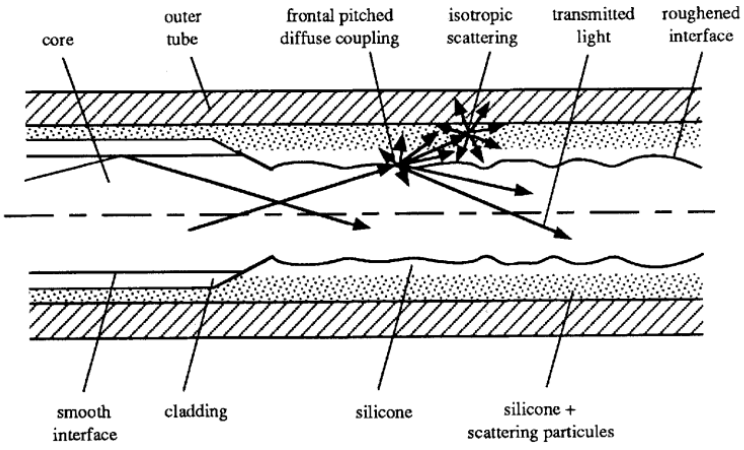


**Figure 4.2:** Radial coupling diffuser obtained by light scattering in a $TiO_2$ loaded polymeric external layer.

An interesting light diffusing tool is the balloon diffuser, applied in interior tissue surfaces irradiation, for example larynx or esophagus. It consists of a cylindrical or linear diffuser inserted into a balloon then filled with a liquid scattering material, providing uniform irradiation of the surfaces and a more efficient light delivery [10].
Some examples of the listed diffusers are shown in figure 4.3.

Fiber diffusers can be also fabricated using femto-second lasers inscription, writing localized refractive index variations in the fiber, creating complex structures able to deflect and scatter light out of the fiber. The great advantage of these kind of manufacturing is that the resulting fiber does not lose its mechanical properties given that the fiber physical structure remains untouched. In this way, the resulting tool maintains its original flexibility and resistance, delivering quite high powers with customized emission profiles

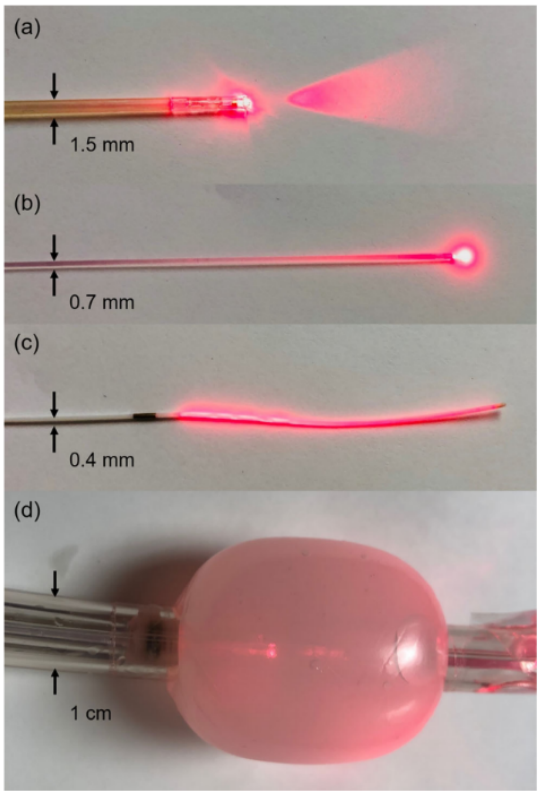


**Figure 4.3:** Fibers with (a) microlens, (b) spherical diffuser, and (c) cylindrical diffuser. (d) Balloon applicator with fiber surrounded by scattering medium.

based on the kind of structure inscribed in the fiber using the femto-second laser. The irradiation profiles obtainable are plenty, including forward, lateral and cylindrical emission.
Many of these structures have a symmetrical shape to provide a uniform all-around light distribution. To do so, the femto-second laser has to be equipped with a rotating holder that rotates the fiber during the inscription, creating for example a spiral or cylindrical inscription shape (fig. 4.4).

Alternatively, linear structures can be impressed in the fiber core, if the rotating stage is not available. This procedure adds some complications due to the difficulty of obtaining a symmetric irradiation profile with a structure that is not symmetric on all the three dimensions. Figure 4.5 depicts the region of the core where the inscription takes place, and shows how the spots, created by the laser, overlap, creating a complex structure with squared cross section [11].

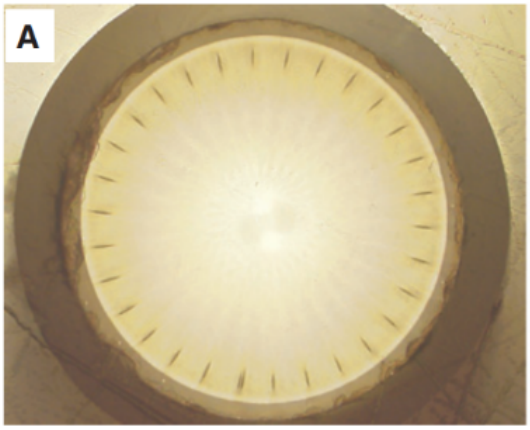


**Figure 4.4:** Fiber diffuser inscribed with femto-second laser machining of a cylindrical structure.

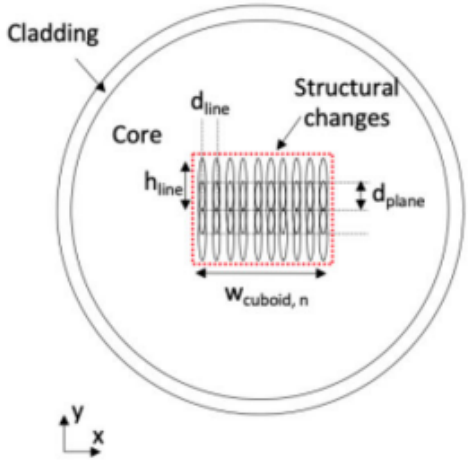


**Figure 4.5:** Cross section of a diffuser inscribed without rotating the fiber. The complete structure is composed of many "cuboids", blocks with a refractive index variation with progressively wider dimension.

## 4.2 Uniformity characterization

The characterization of the light emission profile is a basic requirement when evaluating the characteristics of a diffuser. The radiation should be scattered out of the fiber in the most controlled way, following the constraints studied and described in the design. The emission profile does not have a unique

reference standard, and based on the application many diffusers can be procedure, from lateral and unidirectional emitters to all-around and homogeneous diffusers.
In many medical applications, a uniform radiation diffusion could be of interest to produce equal results on the region under treatment, hence the necessity of performing the uniformity characterization of the diffusing device. In order to evaluate the emission profile of the diffuser, two methods could be implemented following a theoretical and an experimental procedure.
A preliminary way to study the emission results of the diffuser is to resort to a 3D ray tracing tool with a proper implementation or numerical simulations. These kind of program has been used to study the beam profile of spherical, tapered and hemispherical tips [12]. Experimentally, uniformity can be measured trough imaging methods, such as a camera, or non-imaging methods, like using a photodiode or a silicon detector. Both the alternatives are based on the possibility of rotating the fiber with a fixed angle step, measuring the longitudinal emission profile for many orientations, then deriving the complete irradiation map of the diffuser. During the measurement, it is possible to move the detector along the fiber, to retrieve the point-by-point values of the emitted power [11, 13].
Both the imaging and non-imaging methods are carried out in [11], where the diffuser created through femto-second laser inscription exhibits an emission efficiency $\epsilon$=(81.5±5.9)%, an intensity variability of (19 ±5)% between distal and proximal diffuser end (fig. 4.6), with a maximum diffused power of 15 Watt without harming the device itself.

## 4.3 Power dissipation evaluation

One of the crucial parameters that define the quality of the diffuser is the emission efficiency, that is calculated as the power dissipated by the diffuser with respect to the total input power sent in the fiber:

$$\epsilon = \frac{P_{diff}}{P_{total}}$$

The emission efficiency parameter can assume any arbitrary value, varying on the application proposed. The same does not apply to the total power emitted by the diffuser, since an arbitrarily high or low power can compromise the outcome of the therapy.
For example, an high power entering a small, highly emitting diffuser generates an high power density on the surface of the emitter, risking to burn the fiber's polymeric coating or damage the exposed tissue. Vice versa, a low power

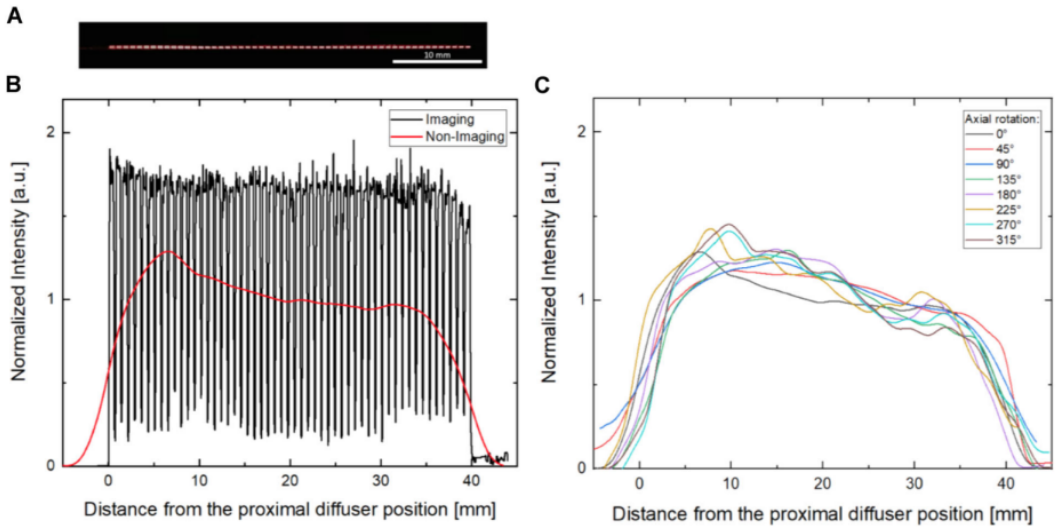


**Figure 4.6:** (A) Image of light distribution on the surface of glass fiber, coupled to a laser light source on the left, recorded with the imaging method. (B) Axial Emission profiles were determined with the imaging method (black) and the non-imaging method (red).(C) Emission profiles for eight different azimuthal rotation angles from 0° to 315° in steps of 45° around the diffuser's z-axis. The profiles were recorded using the non-imaging method.

injected in a long diffuser with small emission efficiency will correctly spread and deliver the power on the outside tissue, but the energy density will be too low to trigger any photo-chemical response from the photosensitizer. Moreover, having a diffuser with small emission efficiency means that the input power is not completely emitted by the diffuser, remaining in the fiber and exiting from the tip, again creating a small light spot with high power density, that could be an issue during interstitial treatments.
The experimental evaluation of the emission efficiency $\epsilon$ is performed measuring, using a photodiode or a power meter, the total power emitted by the optical fiber with the diffuser attached to it, obtaining the remaining power that is not emitted by the diffuser. Afterwards, the diffuser is removed and again is measured the power coming out of the tip of the fiber, that is equal to the input power delivered to the diffuser; the emitted power can be obtained subtracting the two power values measured experimentally, and the emission coefficient is the ratio between this value and the total power at the input of the diffuser. (Fig. 4.7)

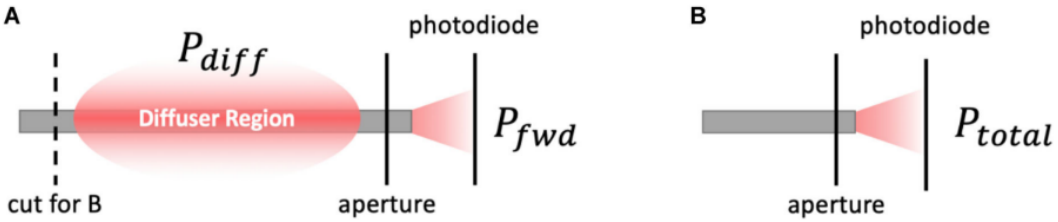


**Figure 4.7:** Schematic representation of setup used to measure the emission efficiency of light emitted from the diffuser. (A) Measurement of the power fraction $P_{fwd}$ not emitted by the diffuser (B) Measurement of the power $P_{total}$ propagating in the fiber before entering the diffuser region.

## 4.4 Diffusers with temperature sensor integration

The idea of developing a smart probe with an integrated temperature sensor comes from the need of monitoring in real time the effects of the therapy, locally measuring the temperature variation in the irradiation site, that is a key parameter in many medical procedures, such as PDT and, mostly, PTT. Moreover, using probes with integrated sensing systems allows to limit the invasiveness of the therapy, reducing the number of probes needed to monitor and collect data about the progress of the treatment.
The general concept is to exploit the properties of the fiber Bragg gratings, inserting an FBG-based temperature sensor inside the diffuser. The FBG is written, as already described, through he local and periodic modification of the refractive index of the fiber core using a femto-second laser machine. The FBG machining should be done such that there is no interaction or distortion between the inscription made to create the sensor and the ones needed to develop the diffuser. Furthermore, the two light beams needed to interrogate the FBG sensor and irradiate the external tissue have different characteristics, since the FBG interrogation is performed at very low power with an incoming, broad spectrum irradiation. On the contrary, in PDT, the diffusing radiation should be at the exact wavelength needed for interacting with the PS and a power high enough to activate it, meaning that the light beam should be more energetic with respect to the sensing one.
All these necessities bring to the conclusion that a typical single-mode fiber in not sufficient to satisfy all the requirements, needing a more complex structure to implement all the features. It has been proved that an FBG system can be integrated in a delivery device based on a Double Cladding Fiber (DCF), where the FBG sensor is placed in the core of the fiber, while the irradiation

beam is carried by the inner cladding [14].
The simultaneous excitation of the core and inner cladding of the fiber has to be performed through a suitable combiner, able to collect multiple light beams from multiple fibers and combine them in a single output. Regarding the needed application, the sensing beam should be coupled to the core of the double cladding fiber, while the diffusing light needs to be injected in the inner cladding. Hence, one of the input fibers should be coupled just to the fiber core, while the others are coupled to the inner cladding of the DCF.
Differently from the cladding of a single mode fiber, the inner cladding of the double cladding fiber has guiding propertied thanks to the present of the outer cladding that, due to a different refractive index, satisfies the total internal reflection condition, confining light in the inner cladding and creating two coaxial waveguides. In order to obtain light emission, a possibility is to phisically modify or scratch the outer cladding, as shown in figure 4.8.

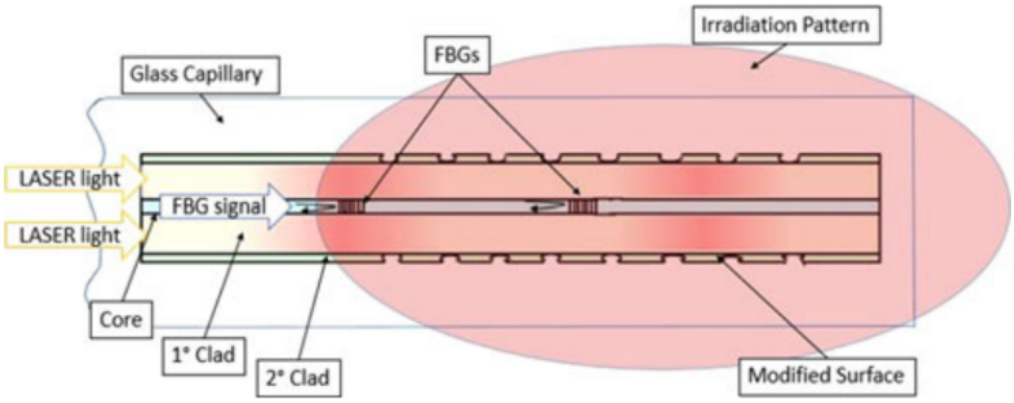


**Figure 4.8:** Schematic representation of an integrated fiber probe with temperature sensing and light diffusing properties. The picture shows the structure of the fiber and the presence of FBG sensor in the core, while the laser light travels in the inner cladding. The glass capillary is present to protect the fiber tip from possible damages and to present its optical properties when inserted in aqueous media.

# Chapter 5

# Design of the diffuser

The aim of this Master's Thesis is the development of a fiber optic cylindrical diffuser that can be then combined with fiber Bragg gratings for sensing the induced temperature and obtain a smart applicator for interstitial photodynamic therapy.
The preliminary studies regarding the diffuser fabrication suggest that its best implementation includes the implementation of light delivery through optical fibers and the manufacturing of the distal end of the optical fiber to achieve light emission, including the femto-second laser machining of the fiber tip to create ad hoc structures with modified refractive index. In this way, light emission is achieved without physical damaging the fiber structure and ensuring the preservation of its original mechanical properties, such as mechanical resistance and flexibility.
Maintaining the mechanical and physical properties of the optical fibers is a crucial aspect in the creation of a diffuser for medical application, whose aim is to be applied in very sensitive areas in which is necessary to avoid any risk of breaking the fiber or the diffuser, both for the danger of creating sharp glass edges that may lesion the tissues and for the possibility of inducing an unwanted concentrated light emission from the fiber, generating high power density regions that could lead to damage or burn the healthy tissues.
The emission efficiency measurement and uniformity characterization are also performed. The emission efficiency is evaluated using a photodiode-based power meter, while the uniformity characterization needed the creation of a dedicated set-up, including a phantom made of ink-loaded agar gel, designed to mimic the properties of a biological tissue, and a set of FBG arrays for temperature measurements.

## 5.1 Choice of the starting sample

The first question to be faced is the choice of the fiber that will be used to fabricate the diffuser. Among the many types of available fibers, a SMF28 fiber and a double cladding fiber have been selected. The SMF28 has the advantage of having a simple structure and more predictable behaviour in terms of excitation, since light travels only in the core. Double cladding fibers are more versatile, opening the possibility to different fabrications and FBG integration, having two propagating regions in their structure; however, the more complex structure may generate problems in terms of light propagation and cross-interference when exciting the propagating modes. Moreover, to exploit the possibility of separately exciting the two guiding cores a suitable combiner is needed.
In conclusion, SMF28 fibers could be used for the initial prototyping of the diffuser, trying to understand and write complex structures to be then implemented on the double cladding fiber, that is the most suitable to implement the final design of the diffuser with sensing capabilities. In the practical experimental tests, the starting point has been the direct writing of the double cladding fiber, since the structures tried to fabricate were rather simple.
There is another requirement that has to be considered while choosing the fiber sample to use, and it is the diameter of the fiber. In principle, a fiber with larger dimensions is usually more resistant to bending and stretching, making it a more suitable candidate for medical procedures in order to preserve the patient's safety during the operation. Indeed, many fiber-based diffusers are built using fibers with 400 µm of diameter. This kind of sample could not be used in the available femto-second laser due to a lack of holding components of the correct dimension, hence this type of diffuser was not fabricated.

## 5.2 Femto-second laser fabrication

Following the design principles explained in chapter 4, the most promising fabrication technique stands in the use of a femto-second laser, inscribing a local variation of the refractive index of the fiber in order to achieve the desired diffusion profile writing a particular structure. Obtaining a uniform emission may be easier designing a symmetric rotational structure in the fiber core. Despite this, the available femto-second laser was not equipped with rotational stages, hence the fiber could not be rotated during the inscription, impeding the creation of rotational structures.
Longitudinal and azimuthal components had to be experimentally related to the linear inscriptions producible, in particular to the different parameters

that characterize any femto-second laser inscription: laser power, inscription trajectory, length and position of the inscription. A standard choice that has been made is that the diffuser length is of 3 cm, that is the maximum available length for the inscription of the available fs-laser.
Regarding the structure to be inscribed, the decision was to start by understanding how a simple, linear and high power inscription in the inner cladding of the fibers scatters light. The result produced is said to be a "damage", because writing a structure with this parameters in the fiber core would decouple all the light out of the fiber, as a physical damage would do. The structure can be freely varied, for example changing its position (near or far from the core), trajectory (parallel to the core or tilted) or dividing it in more segments with different characteristics, even by placing them on different sides of the fiber (such as top and bottom).
Even if the damage has to be performed at high power, the exact value can be tuned and changed trying to understand which power values/profiles give the best results in terms of uniformity of the emission. Moreover, the system is equipped with two variable attenuators that must be both properly configured to obtain the desired power level.

## 5.3 Homogeneity evaluation

The evaluation of the azimuthal and longitudinal emission components is the most meaningful measurement when characterizing an optical diffuser. Given that the device is studied for interstitial PDT application, the desired emission profile should be as uniform as possible over the whole irradiation volume, both from the sides of the fiber and from the tip, or at least it should avoid the overexposure of a portion of the tissue, such as the non-diffused light exiting from the fiber tip. The shape of the irradiation volume should be then as close as possible to a cylindrical shape, with uniform power distribution both along and around the fiber.
As a preliminary hypothesis, the expected result of a uniform and linear femto-inscribed damaged is a variable power emission profile, with higher light diffusion at the beginning of the diffuser. This prediction comes from the simple fact that a uniform structure written in the fiber will always scatter the same portion of light in every point, but the input power of every localized damage decreases as light travels inside the diffuser due to the scattering effect that the preceding portions of the diffuser have already applied. Therefore, in order to obtain a uniform emission profile, this effect should be compensated.
Experimentally, the homogeneity evaluation has been performed using two

different set-ups, one to primarily evaluate the longitudinal emission of the diffuser, the other to effectively study the shape of the irradiation volume and the power emitted in different directions.

### 5.3.1 Camera set up for longitudinal characterization

The first evaluation method is performed using a **camera** (CC3260C - High-Resolution USB 3.0 CMOS Camera, Thorlabs) that acquires black and white images over a wide wavelength spectrum, including all the visible region and part of the near-infrared spectrum. The image given by the camera shows white pixels for high light intensity regions, where the brightness of the pixel's color can vary on a scale form 0 to 4095, with the possibility of adapting the software acquisition parameters in order to obtain brighter images by modifying the optical gain or extending the acquisition time.

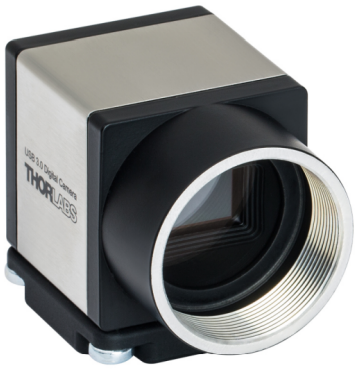


**Figure 5.1:** Photo of available camera, taken from the quick start guide present in the Thorlabs website.

The downside of this camera model lies in the lack of an adjustable focus, needing a system of collimating lenses to focus the incoming light in the objective of the camera. Moreover, once the lens has been mounted and the sample is correctly visualized by the camera, neither the sample nor the camera should be moved anymore, causing problems when trying to substitute the samples and collect their images one at a time. The lens selected has a 35.00 mm focal distance, with some complementary tubes to correctly space the lens and the camera objective (fig.5.2). The lens is provided with a BBAR coating 400-700 nm. The distance at which the image is correctly focused by the camera is around 13 cm.


**Figure 5.2:** Picture of the camera and lens set-up.

The camera functionalities are exploited through the ThorCam software using the provided USB cable to control the camera from the user's PC. The software used for the image acquisition is equipped with the possibility of drawing the plot of the intensity of the pixels for any chosen line or column, producing a more quantitative analysis of the light distribution of the diffuser. This feature is able to select just a line of pixels, but for a more precise analysis it could be useful to equip the possibility of selecting multiple lines of pixels and make their average intensity. This feature has been developed through a MATLAB script, that analyses the .png format of the exported image taken by the camera and evaluates the intensity of multiple pixel lines or columns. The light emission from the diffuser was obtained connecting the diffuser to a low power He-Ne laser or to a commercial fiber checker.

### 5.3.2 Image analysis

A typical image obtained using the camera is presented in figure 5.3, that is a screenshot taken from the ThorCam software, using one of the fabricated diffusers as subject of the picture. The distance between the camera and the fiber have been adjusted to produce the best focus for the image, and the fiber has been placed on a rigid support to keep it stretched.

The longitudinal analysis can be performed by the software itself using an apposite function, that traces a plot of the brightness of the pixels both vertically and horizontally, but just for one line. In picture 5.4 is shown an example of this procedure, using the same photo of figure 5.3.

Carefully looking at figure 5.4 it can be seen that the red line and the diffuser

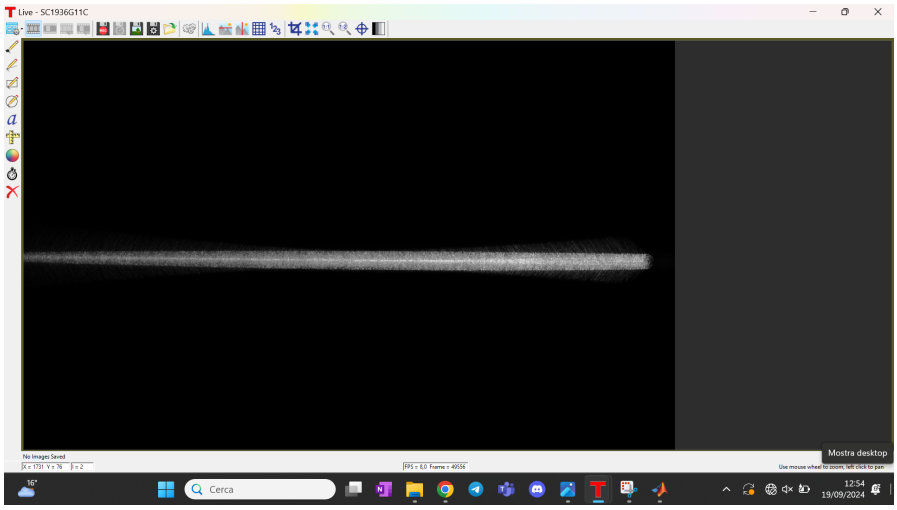


**Figure 5.3:** Picture of a diffuser as taken by the camera.

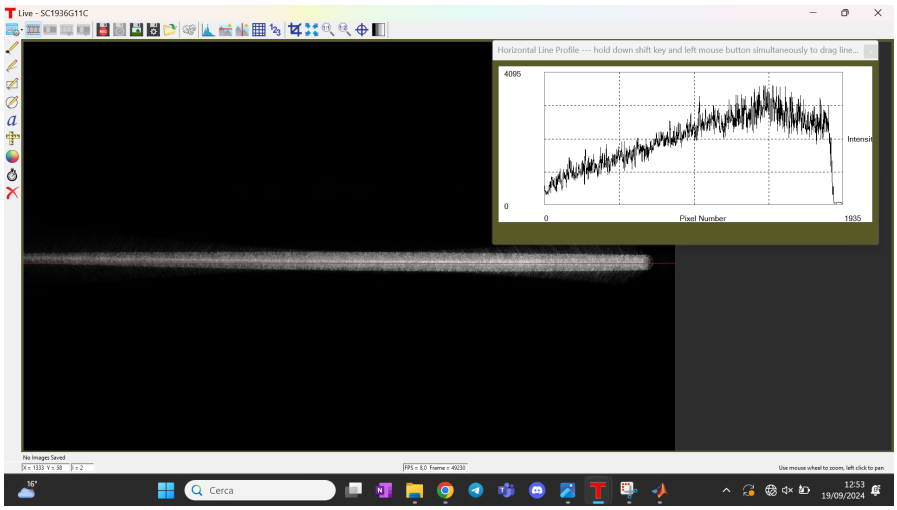


**Figure 5.4:** Example of pixels brightness analysis performed by the software. The selected line of pixels is colored in red.

shape are not perfectly aligned, giving a sort of offset error to the intensity analysis. This result can be compared to the intensity profile given by the MATLAB code in fig. 5.6, showing good similarity in the intensity profiles for two graphs. The MATLAB analysis is performed selecting five lines of pixels, but the number can be selected as desired. The vertical axis in figure 5.6 is scaled to 250 instead of 4095 due to the file format that MATLAB elaborates.

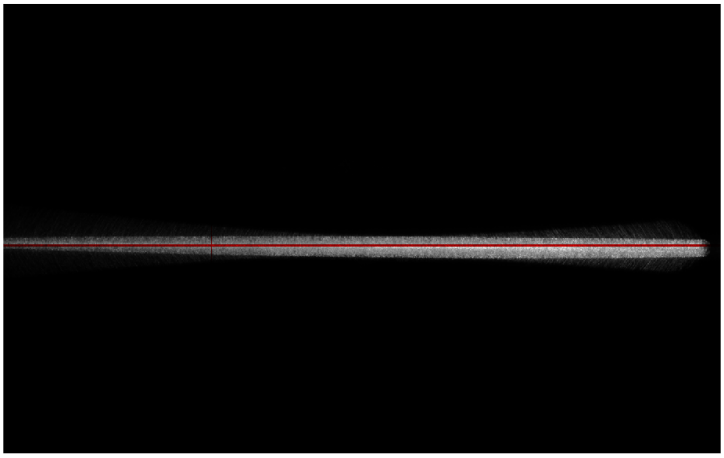

**Figure 5.5:** Pixel lines considered by the MATLAB software to perform the intensity analysis.

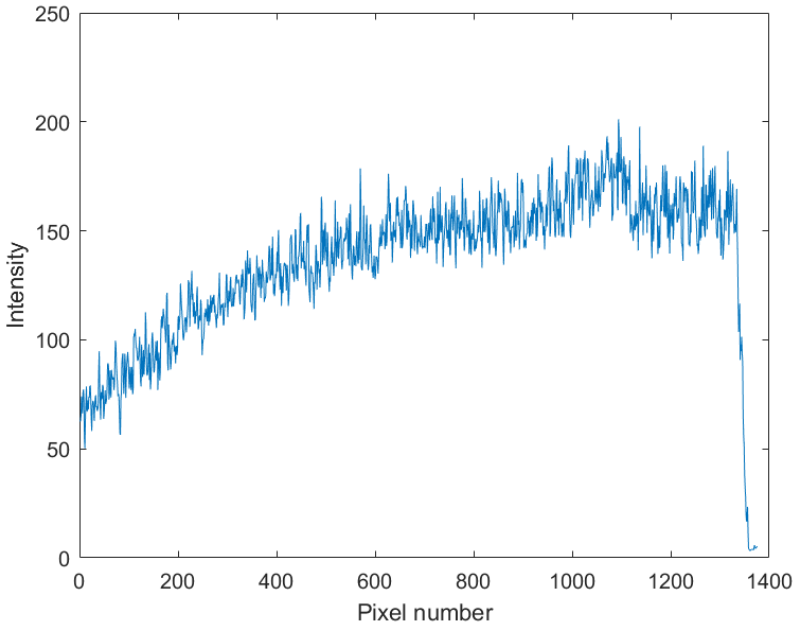


**Figure 5.6:** Plot of the pixel intensity, averaged for the selected lines.

### 5.3.3 Tridimensional uniformity of the emission

The second set-up implemented to measure the volume uniformity of the emission and its details are further explained in chapter 6, where the characteristics of the single building blocks are better specified, showing the reasons and needs that drove the different choices. Here, the explanation will regard the general scheme implemented and the main idea behind it.
The first consideration to be made is how to measure the emission profile of the diffuser. The solution could be using some kind of photodiode able to collect the light emission at 360° around the diffuser and along the whole fiber length. This kind of device was not available, so a different solution had to be found. Instead of directly measuring the radiation, it may be possible to measure the temperature generated by the light dissipation in a block of absorbing material, using just some temperature sensors, relating the heating profile to the radiation diffusion profile.
This kind of measurement would require a particular kind of sensor able to perform localized and multi-point measurement, such as an FBG array, that is a sequence of FBG sensors all placed on the same fiber at arbitrary distance one from another and with very short length ($\sim$ 2 mm). The advantage of this kind of sensor, besides their precision and sensitivity, is the possibility of performing point-by-point distributed sensing, thanks to the small dimension of the FBGs that can be approximated to a single point and their variable distance, properly designed to measure a particular temperature profile.
Once that the sensing system has been chosen, the next step is to find a suitable material, that has to be a solid material with strong absorption in the visible and near-infrared optical windows and, ideally, common optical properties with the biological tissues. Many researches have shown that the Agar Agar gel satisfies these properties, and to give it stronger light absorption coefficient it can be loaded with a small quantity of black ink.
In conclusion, the basic set-up can be described as follows: the diffuser is inserted in an ink loaded agar gel block, surrounded by the arrays of FBG placed at a fixed angle one from the other and at a fixed distance around the central diffuser. A light beam is injected in the diffuser, that scatters away the optical power towards the external of the fiber, in the agar block. The radiation is taken up by the material that starts heating up proportionally to the quantity of absorbed radiation. The temperature change is then measured in real time by the FBG sensors placed around the fiber and, knowing the position of the sensors, it is possible to obtain the temperature profile inside the agar block, and consequently the radiation profile. The final goal is obtaining a uniform distribution profile, that is when the FBG-based sensors indicate the same temperature across the whole volume at every time instant.

## 5.4 Measurement of the emission efficiency

The experimental evaluation of the emission efficiency is performed as explained in chapter 4.3. Practically, the two powers $P_{diff}$ and $P_{total}$ have been measured using the power meter, collecting the power coming out from the tip of the fiber. In the first case, the diffuser was attached to the fiber, while in the second the diffuser has been cut-off.
A practical aspect to be considered is the following: the bare fibers are commercially available with length of tens of meters, from which the user can cut the desired length for the application needed. These fibers need to be splice to a suitable pigtail element, that is responsible for the light coupling between the device output connector and the fiber. A splice is performed by simply fusing and joining the silica of two fiber tips using a device called splicer, that first performs the alignment and then the splicing procedure. The result is a unique fiber in which light can travel without major losses, with the exception for the segment where the splice is present. Here, light is partially scattered out of the fiber due to non perfect alignment or imprecision in the splicing process. The splice segment is also the most delicate point of the fiber and the easiest to brake.
This power loss has to be considered while characterizing the emission efficiency of the diffuser, because the total power emitted by the laser source is partially lost due to the splice and partially scattered out by the diffuser. The power $P_{out}$ measured as first step for the $\epsilon$ evaluation will be the total power emitted by the source ($P_{source}$) minus the power lost in the splice ($P_{splice}$) minus the contribution of the diffuser ($P_{diff}$), resulting in

$$P_{out} = P_{source} - P_{splice} - P_{diff}.$$

Now, care must be taken when removing the diffuser to measure the $P_{total}$ component -that is the input light entering the diffuser- since it is not sufficient to separate the two fibers in the splice segment, because the $P_{splice}$ component would be removed when calculating $P_{total}$, leading to $P_{total}$=$P_{source}$ and to

$$P_{diff}^{splice} = P_{total} - P_{out} = P_{total} - (P_{source} - P_{splice} - P_{diff}) =$$

$$= P_{total} - (P_{total} - P_{splice} - P_{diff}) = P_{splice} + P_{diff}.$$

The calculation would result in a remaining component given by precedent presence of the splice that introduces a spurious loss. Instead, to correctly calculate the $P_{diff}$ component is necessary to cut the fiber between between the splice and the diffuser, leading to the measurement of $P_{total}$=$P_{source}$-$P_{splice}$,

canceling the contribution of the splice since the total power at the beginning of the diffuser already incorporates the splice loss. The sum of the total contribution is then

$$P_{diff}^{splice} = P_{total}^{splice} - P_{out} = (P_{total} - P_{splice}) - (P_{source} - P_{splice} - P_{diff}) =$$

$$= P_{total} - P_{splice} - (P_{total} - P_{splice} - P_{diff}) = P_{diff}.$$

After the needed measurements, the emission efficiency $\epsilon$ is calculated as

$$\epsilon = \frac{P_{diff}}{P_{total}}$$

The current and power values used during the experimental characterization has been chosen to provide enough power to turn on the laser diode, but not too high in order to avoid a too high exposition of the coating and the splice to the radiation, resulting in the coating starting to burn or the splice breaking.

# Chapter 6

# Experimental set up for homogeneity evaluation

## 6.1 FBGs array sensing system

### 6.1.1 Interrogation of the FBG

In order to acquire data from an FBG-based sensor a suitable device is needed. The working principle is based on the interrogation of the FBG behaviour with a focus on the shift of the Bragg wavelength, done by inserting a broadband signal (generated by a broadband source or a tunable laser) with uniform power inside the fiber and collecting its reflection form the FBG. The reflected wavelength with the highest intensity is the Bragg wavelength because it coincides with the peak reflection of the FBG. The instruments used to perform this task are called optical interrogators, that performs both the actions required. For this particular set-up, a Micron Optics HYPERION si155, by Luna Technologies®, was available. The technical specifications are:

- Wavelength range: 1500 nm - 1600 nm
- Wavelength resolution: 10 pm
- Maximum acquisition rate: 1 kHz for peak detection, 10 Hz for spectrum detection;
- Number of channels: 4, working in parallel
- Dimensions: 20.6 cm × 27.4 cm × 7.9 cm / 3.0 kg.

For this instrument, the detection of the Bragg peak wavelength is automatic for every FBG, and every channel can correctly find up to 20 peaks. The

data processing is simultaneous with respect to the data acquisition, allowing real time measurement of the wavelength shift due to strain or temperature variations.
The general scheme of the instrument is depicted in figure 6.1. The tunable laser continuously swipes all the available spectral range, with the laser emission passing through an optical circulator before reaching the FBG, where just the $\lambda_B$ component in back-scattered. The signal comes back in the circulator and is sent towards a photodiode, that anlyzes the intensity of the signal. The acquisition chain is terminated with an analog-to-digital conversion system. The advantage of this acquisition system is the absence of a tunable filter before the photodiode, since the wavelength selection is already performed by the source. The tunable filter is needed when working with broadband sources, such as super luminescent leds (SLED). The presence of the circulator is essential do separate the forward and backward propagating components of the light signal.

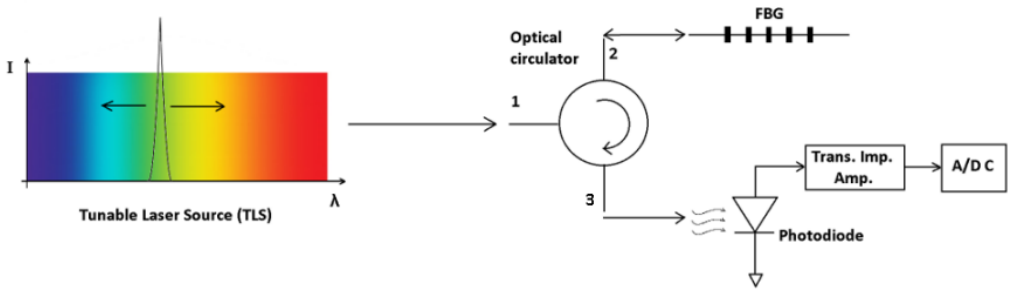


**Figure 6.1:** Schematic view of an interrogator working principle, provided with a tunable laser source.

### 6.1.2 Geometrical parameters of the FBG arrays

The FBG arrays mentioned in chapter 5 are produced with the already described femto-second laser machine and can be manufactured as wished. The main requirements for these sensors is the capability of performing temperature measurements in selected locations, such that the acquired data are meaningful while reconstructing the 3D diffusion map of the radiation. The choice of crafting 3 cm diffuser is a constraint for the system, meaning that the dimension of the arrays should be comparable with this one.

The final design of the sensing system is composed of four arrays of FBGs, each one made of eight single FBGs. The FBGs are 2 mm long and separated by a 2 mm space, for a total length of 3 cm. The Bragg wavelength separation among the FBGs in a single array is of 4 nm, taking $\lambda_B$ values from 1534 nm to 1562 nm.

## 6.2 Alignment of the FBGs and production of the black agar block

The principal issue when trying to mount the set up was how to position the diffuser and the FBG arrays in order to correctly evaluate the light and temperature distribution. The idea of using a solid material such as the Agar gel solved the problem of converting the optical power in thermal heating. However, the critical aspect was to fix the position of the diffuser and the sensors in a stable way, ensuring the alignment among the components. Furthermore, inserting the optical fibers in the agar cannot be done by simply inserting the fibers in the block once it has solidified due to the risk of breaking the fibers and the difficulty of maintaining the alignment while inserting the fiber. The alignment procedure has to be done first, and consequently the agar gel can be poured around the fibers, in a suitable container where it can rest and cure, fixing also the position of the fibers.

### 6.2.1 Agar properties and recipes

The Agar Agar component is commercially available as a white powder and is used for cooking gelatines, such as jelly candies. Despite the preparation of the Agar gel is composed of a few and simple steps, it is essential to list them once to better understand how the set-up in prepared. At first, it is necessary to mix the Agar powder with a small quantity of water proportional to the quantity of Agar gel to be done. The proportion of agar powder and water are not fixed, but they depend on the desired density of the final Agar gel: to an higher concentration of agar powder corresponds a more dense agar gel. The dosage rates indicated on the packaging are 2-10 g per 1 kg of solution, ranging from 0.2% to 1% of agar/water ratio. In the practical preparation of the gelatine, even higher concentrations have been tested to create a more firm gel.
It is then required to slowly bring the solution to boiling temperature, using an hot plate or a stove. Once the water starts to boil, the liquid can be poured in a container where it cools down and solidifies when reaching approximately

40-45 °C. In order to get a black agar block, a small quantity of black oil-based ink is initially mixed to the water and agar solution before starting heating it. An effective recipe used for the proposed set up is the following:

| Ingredient | Quantity |
|---|---|
| Water | 75 g |
| Agar powder | 1 g |
| Black ink | 0.5 g |

**Table 6.1:** Ingredients used in the agar jelly fabrication, with a 1.5% of agar concentration

### 6.2.2 Design of the agar container

The first idea in developing the structure of the agar block was to build a cylindrical structure by casting the agar in a empty glass cylinder, such as test tube. The diffuser could be fixed to stay in the center of the tube, while the FBG arrays were put on the surface of the agar cylinder one it had been removed from the mold. This procedure presented many complex aspects and was abandoned within a few trials, due to the difficulty of extracting the agar cylinder from the test tube without breaking it and due to the impossibility of fixing the arrays on the very smooth surface of the agar block.
The idea of building a cylinder comes from the fact that it has the same shape of the power emission volume, since a cylindrical diffuser has been tested. Despite this, it is not necessary to have a cylindrical agar block as long as the sensors are disposed properly, placed at the same distance from the diffuser at fixed angles. The following idea was then to fabricate a little box with rectangular base and an open top side, so that it is possible to pour the agar inside. The fabrication is possible using a 3D printer, properly designing the CAD model of the box.
The dimension of the box has been studied to contain the 3 cm diffuser and the fiber sensors on the sides, with a total volume big enough to place all the sensors without using or wasting too many ingredients. The final structure shown in fig.6.2 has external dimesion of 60 mm $\times$ 30 mm $\times$ 25 mm, while the inner hole has dimension of 56 mm $\times$ 24 mm $\times$ 22 mm.

In order to insert the fiber sensors in the box before placing the agar, it was necessary to drill five holes on the side walls of the box, the central one for the diffuser and the other four for inserting the FBG sensors. The four external holes were fabricated at 3 mm from the center, at 90° separation one from the

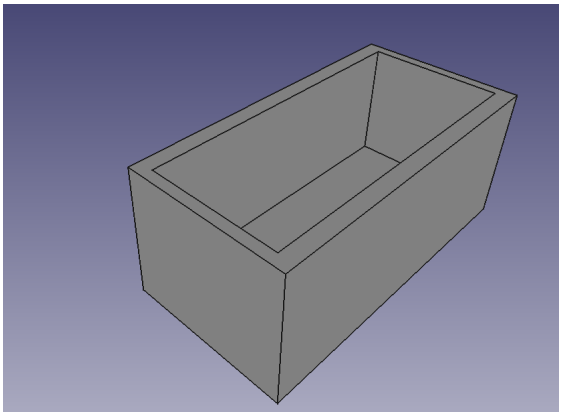

**Figure 6.2:** Screenshot taken from the FreeCAD software that has been used to design the box.

other using a pillar drill.
While mounting the set up, it was needed to keep the fibers as straight as possible so that no bending could be induced in the sensors, mostly due to permanent stress caused by the agar solidification or due to problems during the pouring step. Once the agar had dried up, all the clamps or constraints were removed from the fiber end, to remove any possible source of mechanical stress. This condition is essential to perform a reliable measurement since, as explained in chapter 2.3, any mechanical stress induced on the FBG sensor generates a shift in the $\lambda_B$ that could be mistakenly analyzed as a temperature change.
The last issue to be solved regard the loose fiber ends that remain out of the side walls, because their weight is enough to bend the sensors placed in the box, compromising the alignment among the fibers. However, the fiber ends have to be fixed somewhere, otherwise a simple displacement of one fiber would ruin again the alignment. Considering these two requirements, the conclusion is that the fiber ends cannot be simply glued to the table surface since that would lead to the bending of the fiber deriving from the height difference between the holes of the box and the surface of the table. A smooth slab made of polyurethane was dug in the center to leave room for placing the box, bringing the holes and the gluing point of the fiber ends on the same height level, avoiding the bending of the FBG arrays.

### 6.2.3 Characterization of the box

The dimension of the box is similar to the designed dimension thanks to the high precision of the 3D printer in fabricating a relatively large object. But the

3D printer is not able to fabricate the holes needed to insert the fiber sensors due to the small dimension required and to their position, in the center of the lateral side. It is then required to drill the holes by hand, limiting the precision in the position of the holes and risking to create small misalignment in the fiber sensors. It is required to characterize the measuring system, retrieving suitable calibration coefficients to be applied to the measurements in order to correct possible error sources.
The characterization took place using one of the available diffusers and the fiber sensors, inserting them in the box and covering everything in agar, creating the standard measurement set up. The emission profile of the diffuser is measured a first time in this way, then the diffuser is carefully rotated by 90° and the experiment is performed again, obtaining the emission profile of the rotated diffuser. If the box was perfect, the temperature profile measured in the second case should be the same of the non-rotated diffuser but oriented sideways of 90°. The experiment is performed four times in order to get a full rotation of the diffuser around its axis.
The results clearly show that one of the sensors systematically measures an higher temperature in all the situation, meaning that there is an error in the position of the fiber with respect to the diffuser. Also the other sensors did show an imprecision in the measurement, requiring a suitable calibration, that is done by averaging the temperature shifts obtained by rotating the diffuser, finding the coefficient needed to normalize the temperature profile.

## 6.3 Light source

The last component to be chosen for completing the set-up is the light source used to send the optical power inside the fiber and toward the diffuser. The possibilities depend basically on the type of device, on the output wavelength and on the delivered power, with important care for the type of output connector that the source is provided with.
Regarding the device, the immediate choice was to employ a laser diode instead of a LED thanks to its wider power range and more stable emission. Moreover, the laser is the most used device in medical applications. The output of the laser must be coupled to an optical fiber with standard fiber-end connection, such as a single or multi mode pigtail, avoiding the SMA-type connector that is not compatible with the fibers used to produce the diffuser. Alternatively, and this is the practical case of the experiment, the fiber can terminate with no connection, allowing to directly splice the output fiber to the diffuser.

The output wavelength has been chosen starting from the practical implementations of PDT, that are based on the near-infrared irradiation of the photosensitizer. For comparison purpose, sometimes also a blue laser diode has been used in the experiments.
Considering the power values to adopt, the usual PDT does not need to provide high power values to activate the PS, but this depends on the emission efficiency of the diffuser and on the local power density that is irradiated. Generally, a standard laser diode is sufficient to provide the necessary power. To properly understand the behaviour of the diffuser and the induced temperature change many power values have been tried out, carefully controlling them in order to maintain a low temperature raise in the agar gel to avoid any deterioration of the material.
The selected laser diode was the oclaro BMU25A-915-01-R, a laser diode emitting a radiation around 915 nm, with maximum power of 25 W.

## 6.4 Complete set-up

The scheme of the complete measuring system can now be explained. The fiber containing the diffuser is inserted in the central hole of the box, while the other holes host the FBG arrays, ready to be submerged by the agar gel. The sensors are connected to the MICRON OPTICS through suitable pigtails, inserting one array for every channel of the instrument. The diffuser instead is connected to the laser diode, wired to a current controller that determines its output optical power.
The laser is fed at a fixed current for 30 or 60 seconds, generating a 915 nm radiation that is sent in the fiber, traveling toward the diffuser. Upon reaching the device, light is scattered out of the fiber in all the direction and is absorbed by the black agar block, that starts to heat up. The temperature variation affects the Bragg wavelength of FBG arrays due to the induced strain and refractive index variation of the silica, that is sense by the interrogator trough the analysis of the reflection spectrum of the FBG arrays.

## 6.5 Integrating gold nano-particles

The use of gold nanoparticles is not strictly necessary to perform the experiment, but it is a good method to acquire preliminary data about the interaction between the diffused light and the particles that would be used in a real medical application. The gold nanoparticles have been produced

in collaboration with the Chemistry Department at Turin's University, with the possibility of tuning the characteristics of the nanoparticles by changing the details of the synthesis procedure [15]. In this case, the final product has been studied to get the form of gold nanorods, with dimensions capable of conferring the infrared absorption to the particles.
Experiments have been done testing just a small quantity of gold nanoparticles and water solution in a test tube, studying the reaction obtained in a controlled environment isolating the nanoparticles from possible external agents. Indeed, the final evaluation should be done in a biological tissue that is composed of many inhomogeneities such as layers with different density or the presence of blood vessels that interfere with the light propagation, and the chemical environment present in the human body could deteriorate the nanoparticles. Due to these reasons, a preliminary experiment can be implemented inserting a small quantity of gold nanoparticles in the agar block, enhancing the absorbing capability of the material and increasing the temperature variation at the same power value. The advantage of the agar is to prepare an homogeneous environment with similar optical properties with respect to biological tissues, avoiding problems regarding the chemical interaction.
The main consequences for the integrity of the nano-particles could come from the high temperatures reached while heating the agar/water solution while preparing the jelly. The gold nanoparticles could sustain a temperature increase of some degrees without deteriorating, but reaching 100°C could destroy their properties. The solution is then to mix the nano-particles once the agar has cooled down but not yet solidified, so that the temperature of the agar is much lower and it is still possible to stir the liquid gel, uniforming the particles distribution.

# Chapter 7

# Discussion of the results

This chapter is devoted to the presentation and the discussion of the results, both of the longitudinal analysis and homogeneity evaluation. The study has been performed following the methods presented in the previous chapters, analyzing whether the longitudinal or side emission are reasonably uniform. The different structures explained have been given meaningful names following the geometry inscribed in the fiber. This classification has been done arbitrarily, investigating which aspect of the inscription is more influential on the emission profile and how the inscription parameters can be tuned in order to obtain better results.
The longitudinal analysis and uniformity characterization have not been done for all the diffusers since many of the aspects investigated are presented to solve just one of the two issues, without considering what is happening to the other feature. As a standard, it has been decided to implement the diffuser using a fix laser power value, with the Carbide attenuator value set to 85% and the SCA attenuator fixed at 90%, where 100% means that the laser power is completely transmitted towards the fiber. These values have been proved to achieve power diffusion and are kept constant in the fabrications, if not differently stated, to better compare the different results.

## 7.1 One sided inscription

The first type of structure fabricated is very simple and is represented by a uniform damage along one side of the fiber, written with a constant power and in the same relative position for its whole length. In particular, the inscription is performed at 27.5 µm above the fiber core, in the center of the inner cladding. The result of the longitudinal analysis performed with the

camera set up is presented in figure 7.1, with the incoming light entering the fiber on the right side of the plot.
The image shows how the first segment of the diffuser is able to emit an higher power, that decreases along the fiber. This phenomenon was expected to happen, since a uniform damage should diffuse a constant portion of power in every given point, but a lower power will be available for the last part of the diffuser given that a part of it is no more present in the fiber.

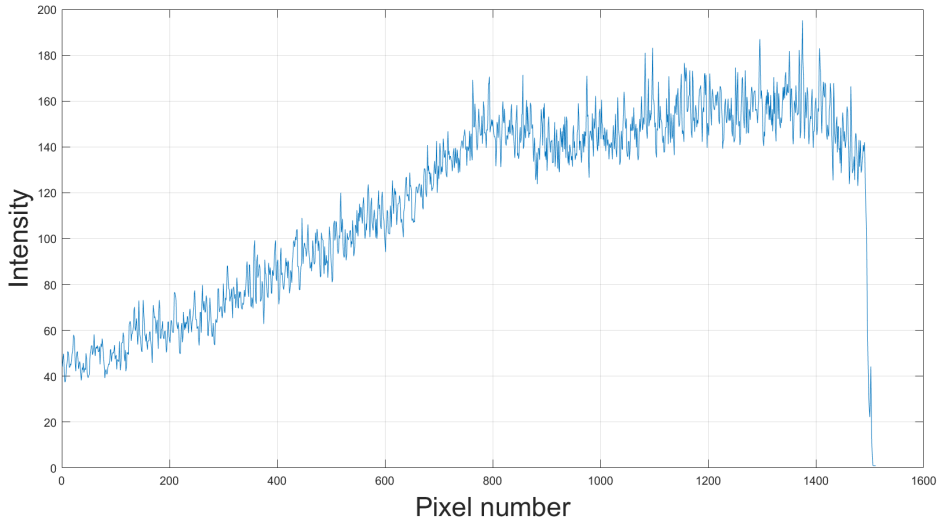


**Figure 7.1:** Longitudinal characterization of the one sided diffuser, performed at 3A input current for 30s.

It is important to underline that the exact value of the pixel intensity is not of interest, and the focus of the analysis is pointed just to the uniformity of the pixel intensity along the fiber length. In any case, the values for the Intensity axis is always presented in arbitrary units (a.u.).

The uniformity characterization presented in figure 7.2 shows how the emission takes place around the diffuser. The plot presents on the y-axis the temperature variation recorded by the FBG sensors, while on the horizontal axis are present the position of the FBG, indicated from 0 to 70, where the 8 FBG sensors are placed at positions 0, 10, 20 and so on. The test has been performed feeding the diode with a 3A current for 30s. The shape of the temperature profiles are very similar, and resemble the shape of the longitudinal characterization done with the camera, with a first part on the right with intense irradiation (and higher temperature generated), while toward the tail of the diffuser the temperature decreases. Again, it is not really important how much the

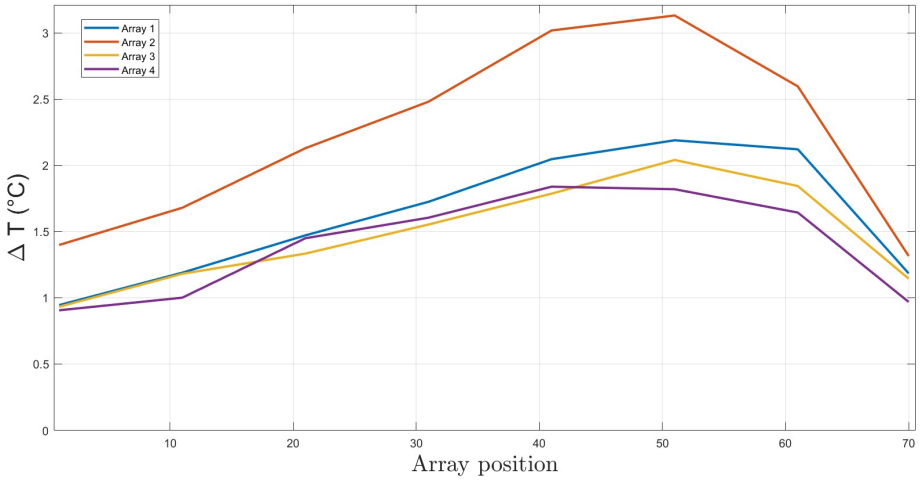


**Figure 7.2:** Uniformity characterization of the one sided diffuser, performed at 3A input current for 30s.

temperature shifted, but rather the relative difference of measured temperature between the sensors.
In this case, the array from number 2 to number 4 seem to measure a uniform profile, with a maximum variation of 0.35 °C around the peak value, that takes place around position 50. Instead, the array number 1 presents a remarkable temperature difference with respect to the other sensors, with a maximum temperature of 3.1 °C, with a 1.1 °C difference with respect to the mean values of the other arrays at position 50, that is of 2.0 °C. This analysis implies that the diffuser has a preferred emission direction, that in this case favored the heat up of the array number 1. This kind of result was again expected since the inscription is done on just one side of the fiber, leading to an intrinsic asymmetry in the damage shape that causes an asymmetric side-emission.
However, it is important to highlight an important characteristic of the diffuser: it is true that the emission is not symmetrical, but still the device works in all the directions, emitting light at 360°. This result is of great relevance because it proves that the side emission is achievable using a simple damaging inscription, at it happens all around the fiber. The following steps will analyze how the inscription can be modified to bring the diffuser to reach a uniform emission on all the sides.
This particular inscription had a little defect taking place during the fabrication, where the fiber was not perfectly positioned and the central section of the damage was written closer to the fiber core with respect to the other parts. It has been studied in the following that a damage produced closer to the fiber

core will diffuse more light, hence the profile of the light emission should be uniformly decreasing along the diffuser length, while in the image 7.1 it seems kind of uniform in the first half of the device.
The emission efficiency characterization has been performed on this diffuser to set a common reference for the other diffusers. The results presented in table 7.1 show that the $\epsilon$ depends on the power values under use, but this phenomenon could also derive from the presence of multiple splices along the optical fiber, inducing higher losses in the propagation path that may depend on the input power.

| Current (A) | Output power (mW) | With diffuser (mW) | $\epsilon$ |
|---|---|---|---|
| 1.5 | 186 | 138 | 25.8% |
| 2 | 550 | 318 | 42.2% |
| 2.5 | 830 | 521 | 37.2% |

**Table 7.1:** Emission efficiency characterization for the one sided diffuser.

## 7.2 Tilted inscription

The purpose of the second kind of inscription produced is the investigation of the influence of the position of the damage on the quantity of light scattered away.
The damage produced is written with an inclination with respect to the fiber length, so that the first points of the inscription are done at the furthest point from the core, while getting closer towards the end of the diffuser. The last points are inscribed in the center of the inner cladding, creating a structure that gets progressively closer to the fiber core.
The result presented in figure 7.3 presents an interesting feature, that is the almost uniform emission from pixels 1300 to pixel 800, keeping an average intensity of 165±30 a.u.
For pixel numbers lower than 800, the power emitted decreases even if the inscription is progressively done closer to the core. This means that the uniform tilt of the damage trajectory is not effective enough to create a strong power emission in the distal end of the diffuser. However, the result seems promising for investigating different sizes of diffusers or creating diffusers combining different inscription techniques.

For this kind of diffuser, the side emission characterization was not performed because the main interest was to understand the variation in the longitudinal profile given by the tilted inscription.

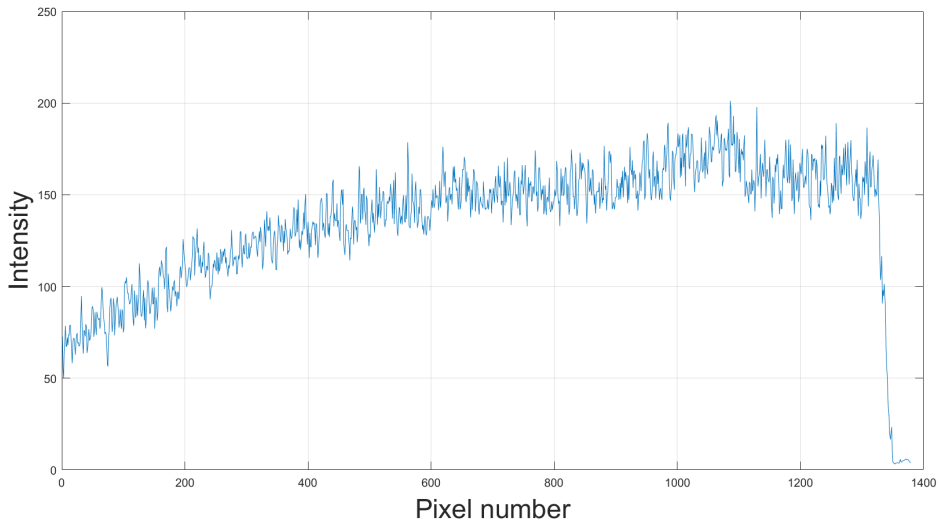


**Figure 7.3:** Longitudinal characterization of the one sided and tilted diffuser, performed at 3A input current for 30s.

## 7.3 Double sided inscription

The following structure analyzed is formed by two uniform damages performed on the opposite sides of the core, both at 27.5 µm from the core boundary. The aim is to understand whether the position of the inscription actually affects the direction of the emission found with the one sided diffuser, or it should be connected to some other aspects of the diffuser machining process. Writing the same damage on two sides of the fiber, the device should diffuse an higher power on two sides of the fiber, leaving the other two almost unvaried with respect to the results obtained with the one sided diffuser.

The result obtained in figure 7.4 does not show the expected result, having just one preferred emission direction as obtained also in the one sided diffuser. The procedure of inscribing the fiber in multiple positions does not solve the uniformity problem, but clearly shows that the temperature raise is much higher in this case with respect to the one sided diffuser, where the maximum $\Delta$T registered was of 3.1°C, while here the maximum of the sensed temperature variation is placed at 7.44°C. Then, the multiple inscription of the fiber on different sides does not affect the lateral power emission, but greatly influences the longitudinal emission profile, increasing the emitted power.

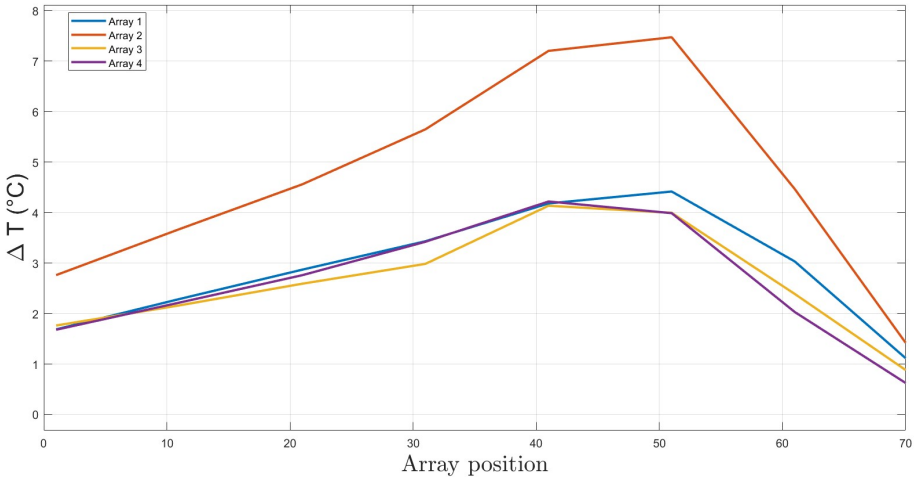


**Figure 7.4:** Uniformity characterization of the double sided diffuser, performed at 3A input current for 30s.

## 7.4 Power increment inscription

Another important parameter to investigate is the power used to inscribe the damage in the fiber. The idea behind the application of a power variation during the diffuser machining comes from the fact that using an higher energy for the UV-laser pulses generates more effective and more visible damages in the fiber, creating a larger modification of the fiber refractive index in a larger spot. The result is an higher scattering power in the diffuser's segments inscribed using more power, and in order to produce a diffuser with uniform longitudinal emission profile a non-uniform inscription is applied.
In particular, the 3 cm structure of the diffuser is divided in six segments of 0.5 cm each, that will be inscribed using different power values for each segment. The power value has been modified only in the SCA attenuator, while the Carbide one has been kept constant at 85%. It has been chosen to modify the SCA attenuator because the attenuation profile is linear and more controllable, while the Carbide power has a non uniform dependency on the attenuator value. Different power profiles have been studied, both with linear and non-linear variations.
The beginning of the test is understanding how a great power variation affects the intensity of the pixels in the photos taken with the camera. The first diffuser fabricated is done with a linear power variation among the segments, starting with a 40% SCA attenuator value and reaching a maximum 90% value for the last segment. The longitudinal profile is presented in figure 7.5, qhere

the input light is given from the right side of the figure, where the 40% power segment is placed. The uniformity is completely absent in this kind of diffuser, but it is very useful to understand how the power values affect the diffusion of the radiation, with the 40% value creating almost no diffusion and with very visible steps in the intensity of the pixels between segments inscribed using different power values.
Another remarkable aspect of this diffuser is that this is the first device whose first segment is not the one emitting the most power, differently from all the kind of devices previously presented. This results hits at the possibility of actually producing a uniform longitudinal diffuser by correctly tuning the power values used in the inscription.

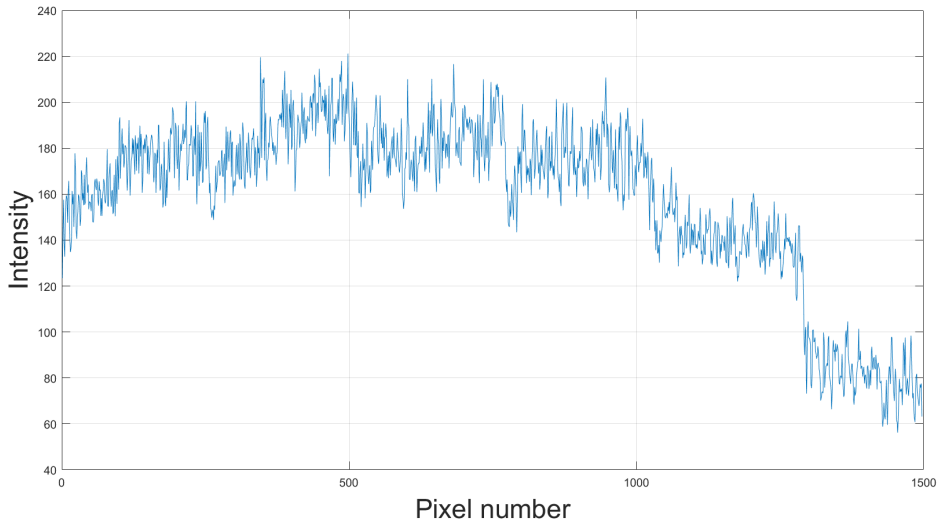


**Figure 7.5:** Longitudinal characterization of the 40-90 diffuser with uniform power profile, performed at 3A input current for 30s.

The second diffuser fabricated with the power variation method aims at decrease the sharpness of the steps present between the different diffuser segments, and the idea is to fabricate the different segments with a smoother power increase along the diffuser length. The two boundaries for the power value are kept at 40% and 90%, but the overall diffuser is written with the following SCA attenuator values, representing one segment each: 40, 45, 53, 63, 75, 90.
The result is reported in figure 7.6 where the intensity profile is still non-uniform but the intensity of the emission gradually increases without taking sharp edges.

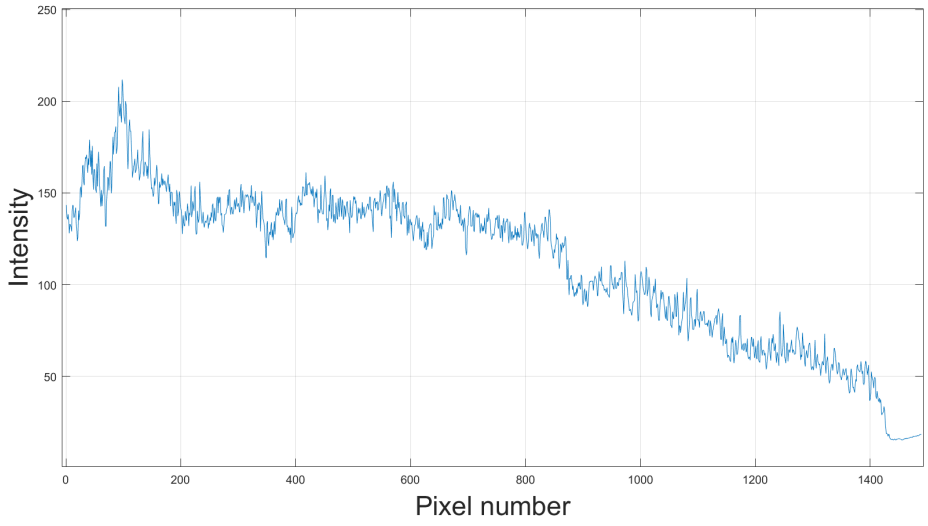


**Figure 7.6:** Longitudinal characterization of the 40-90 diffuser with non-uniform power profile, performed at 3A input current for 30s.

It is now necessary to solve the issue presented in the first segments of the diffuser, where the irradiation provided by the device is too low compared to the emission of the distal end. In order to do this, the approach was to increase the power used to fabricate the first parts of the diffuser, maintaining the smooth power increase presented in the second experiments. Then, the next diffuser presented in figure 7.7 has been fabricated with the following power profile: 50, 54, 61, 70, 81, 95.

The result of this diffuser is quite promising: the intensity profile is much smoother with respect to the previous case and the first segment has an average intensity of 70 a.u., 30% less with respect to the central intensity of 100 a.u., while in the previous case the first segment could emit a 60 a.u. intensity, 60% less compared to the central emission of 150 a.u. The profile uniformity has improved in the new device, but the 360° uniformity has not been tested for these diffusers since this was just a preliminary study about the longitudinal emission profiles.
Some other diffuser have been fabricated trying to correct the initial inhomogeneity of the emission, raising the power value used to fabricate the first segments. For these diffusers, the 360° uniformity characterization has been performed instead of the longitudinal one in order to obtain a more complete information about the shape of their emission volume. In figures 7.8 and 7.9 are presented two diffusers with starting power at 55% and 65% respectively.

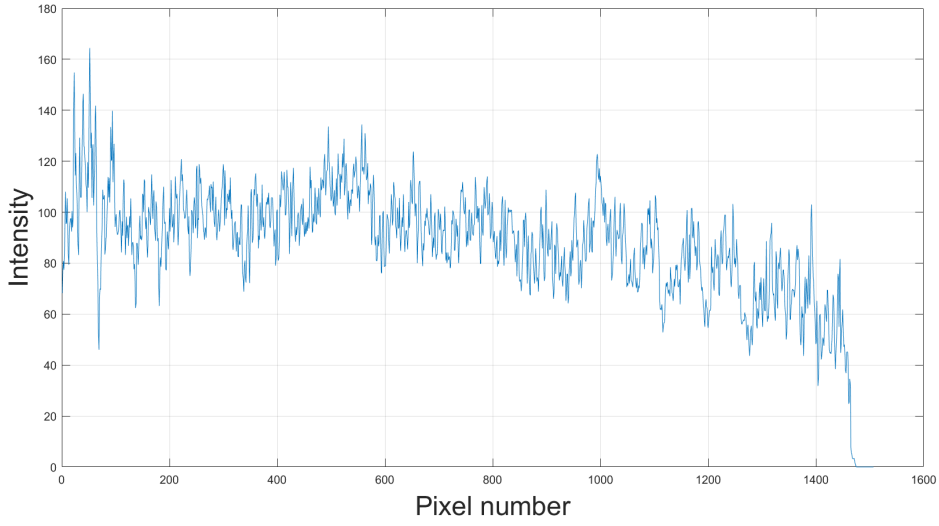


**Figure 7.7:** Longitudinal characterization of the 50-95 diffuser with non-uniform power profile, performed at 3A input current for 30s.

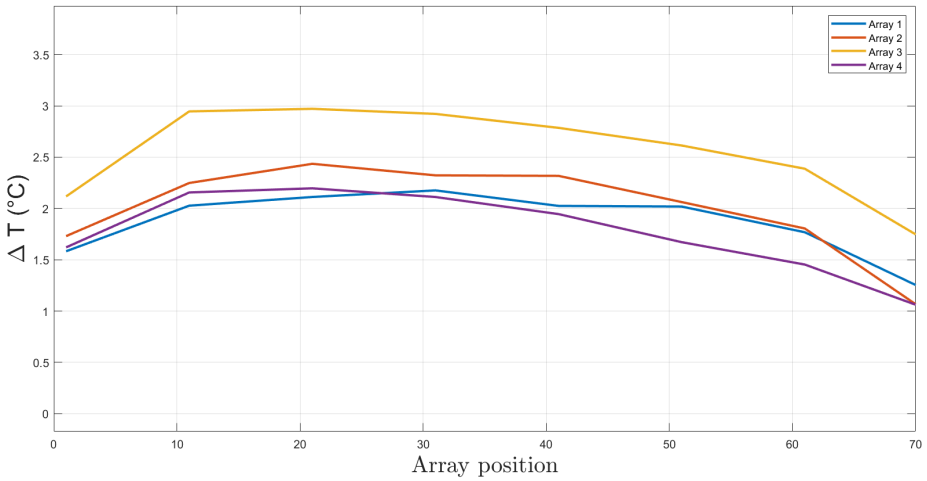


**Figure 7.8:** Uniformity characterization of the 55-91 diffuser with non-uniform power profile, performed at 3A input current for 30s.

These pictures bring to evidence the effect of the power variation during the inscription, resulting in a much more uniform on the longitudinal direction with respect to other diffusers. Considering the positions between 10 and 60, the difference between the maximum and minimum $\Delta$T is around 0.7 °C, within the 30% of the maximum $\Delta$T registered for all the arrays.

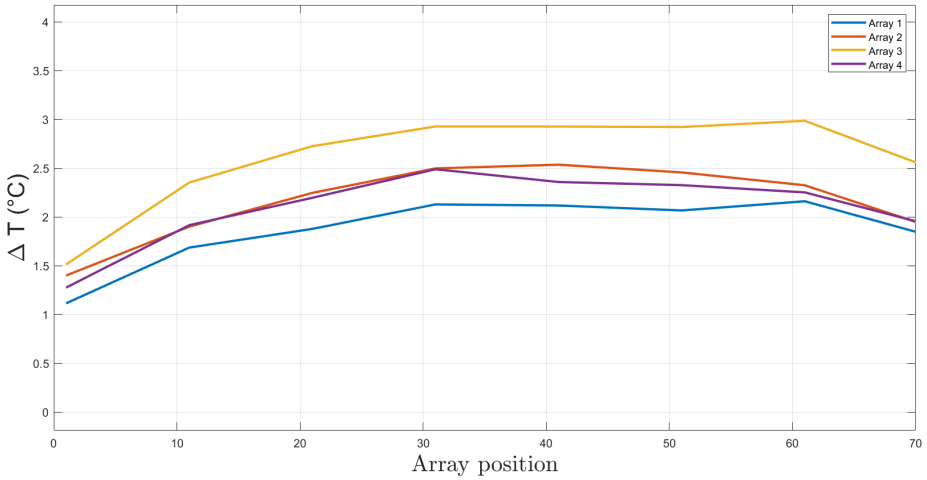


**Figure 7.9:** Uniformity characterization of the 65-93 diffuser with non-uniform power profile, performed at 3A input current for 30s.

Observing the diffuser within the positions 10 and 60, that are the central parts of the diffusers, it is evident that there is still a preferred direction of the emission. By chance, the two plots both show that array number 3 is the one heating the most, but tilting the diffuser towards a different direction also the preferred emission direction changes, heating more one of the other arrays. This simple proof shows that presence of an array heating differently compared to the others is not due to an imperfection of the box but to a non-uniform emission of the diffuser.
However, the difference between the $\Delta$T of the warmer and cooler arrays is always lower than 1 °C for both the arrays (in the same position), that is around a 30% of the maximum temperature, representing an advancement towards the achievement of the 360° uniformity.
In order to derive a more quantitative result, it can be said that considering the position from 10 to 60, the longitudinal variability $V_L$ of the temperature is $V_L$=(22.9±8.4)% for the 55-91 diffuser and $V_L$=(24.5±1.7)% for the 65-93 diffuser, both expressed as percentage difference with respect to the maximum value. For the 360° variability of the emission, it can be calculated that at the same relative position of the FBGs the temperature difference vary in the range $V_{360}$=(32.7±5)% for the 55-91 diffuser, while for the 65-93 diffuser the variability is $V_{360}$=(33±1.5)%, again expressed as percentage of the maximum value.
Acomparison can be made with the diffuser presented above, that had a longitudinal intensity variability of $V_L$=(19±5)% and uniformity of $V_{360}$=(16±8)%.

If the longitudinal variability is similar in the two diffuser, the $V_{360}$ of the reference device is half of the $V_{360}$ of the diffuser under development, meaning that this value should be further studied and improved, creating more complex structures that could uniform the all-around light emission.
As it has been done for the one sided diffuser, in table 7.2 are reported the emission efficiency characterization for these two diffusers. The results show values analogous to the one sided-diffuser, meaning that the power increment does not have much influence on the power emitted by the diffuser.
The values obtained for the emission efficiency are below the expectation,

| Current (A) | $\epsilon$ 55-91 | $\epsilon$ 65-93 |
|---|---|---|
| 1.5 | 25.6% | 27.4% |
| 2 | 32.2% | 36.1% |
| 2.5 | 40.9% | 42.3% |

**Table 7.2:** Emission efficiency characterization for 55-91 and the 65-93 diffusers.

providing an $\epsilon$ well below the 100%, value that in principle should be the optimal target both for avoiding excessive power waste and for guaranteeing the complete emission of the therapeutic radiation. Again, comparing the produced diffuser with the reference, the emission efficiency $\epsilon$=(81.5±5.9)% of the reference diffuser is greatly higher than the one of the diffuser experimentally studied.

## 7.5 Multiple damages inscription

Instead of modifying the power of the inscription, another idea could be to perform multiple inscriptions on the same side of the fiber but at different distances from the core, trying to to improve the diffusion obtained in the final segments of the diffuser by modifying the inner cladding multiple times. The final structure in machined through two writing steps, performed with the same power characteristics used for the one sided inscription. The first inscription is 3 cm long and is performed at 18 µm above the fiber core, while the other is placed at 36 µm above the fiber core and it measures 1.5 cm. The second inscription is placed just in the second half of the diffuser, where the emission should be enhanced to compensate the lower power available for the diffusion. The longitudinal characterization is presented in figure 7.10 and clearly shows the effect of the second inscription, that increments the emission intensity just in the second half of the diffuser (on the left side of the picture), after the step-like behaviour taken by the plot around the pixel number 600.

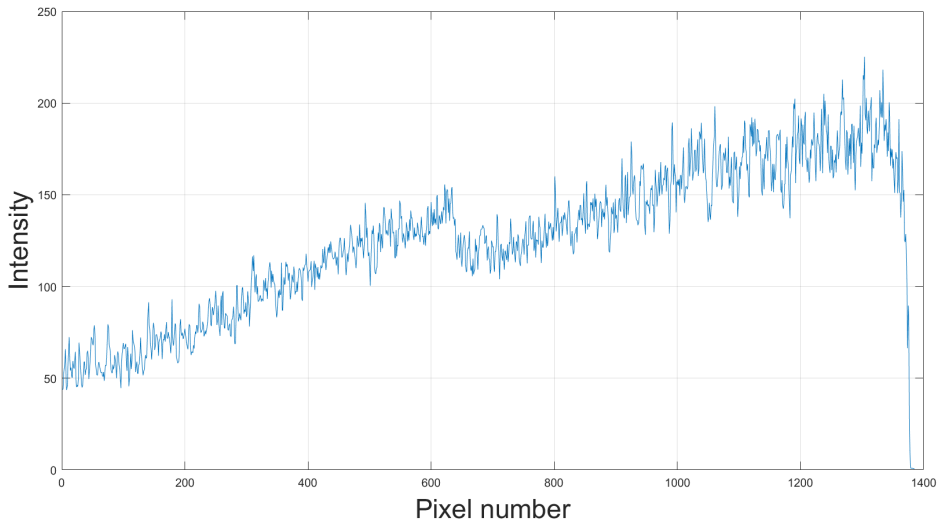


**Figure 7.10:** Longitudinal characterization of the double inscription diffuser, performed at 3A input current for 30s.

The structure can be developed applying a third, shorter inscription on the same side of the cladding, creating a sort of cascade of inscriptions towards the fiber's distal end. The new structure is then composed by three segments placed at 41.25 µm, 27.5 µm and 13.75 µm from the fiber core, with respective length of 3 cm, 2 cm and 1 cm. The obtained intensity distribution is depicted in figure 7.11 and has the same behaviour of the previous structure, with sharp steps at the beginning of a new segment and a decreasing power emission in the other regions. The obtained results show how the presence of multiple inscriptions on the same side of the fiber introduce a too evident variation in the intensity profile for pursuing the aim of a uniform diffuser. Nevertheless, it has been shown that multiple inscriptions do influence each other increasing the emission efficiency, but different geometries and complex structures should be investigated to produce more meaningful results.

## 7.6 The effect of gold nano-particles

One of the most important variation applied to the experiment is the introduction of gold nanoparticles during the agar fabrication. The effect of the NIR radiation on the gold nanoparticles is to generate a temperature raise upon light absorption, and the phenomenon has been studied first in a test tube with different nanoparticles concentration. The preliminary tests evidenced a

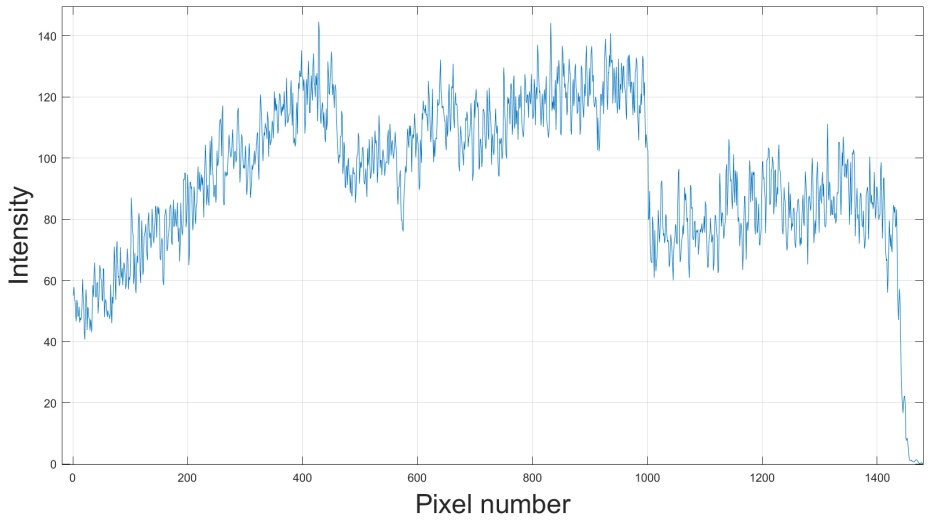


**Figure 7.11:** Longitudinal characterization of the triple inscription diffuser, performed at 3A input current for 30s.

great differnece with respect to the irradiation of the control sample made of water, implying the effectiveness of the gold nanoparticles in producing heat. Inserting the nanoparticles in the agar block, the expected result is to see a larger temperature change upon irradiation, leading to possibility of performing uniformity test with a lower power and for shorter times. The test has been performed using the same kind of diffuser and reproducing the same set up, keeping the same power values and duration for both the experiments. The result are presented in figures 7.12 and 7.13.

The effect of the nanoparticle presence is clearly visible form the difference in the two figures, having an average peak temperature variation of 2.5 °C. at the peak for the agar without nanoparticles, while the other sample presents an average peak temperature varaition of 10.4 °C. The heating produced by the gold nanoparticles is more than four times higher than the one produced by the agar alone, and proves the effectiveness of the procedure.
Actually, looking forward to a PDT application, this result is not actually the desired one: in PDT the temperature of the irradiated sample should stay as stable as possible to guarantee the maximum conversion efficiency in the photochemical reaction and avoiding interference in the treatment given by temperature changes. This result can be explained considering that this particular kind of gold nanoparticles in studied for photothermal application, so the most desired characteristic is actually a high conversion efficiency from light to thermal energy.

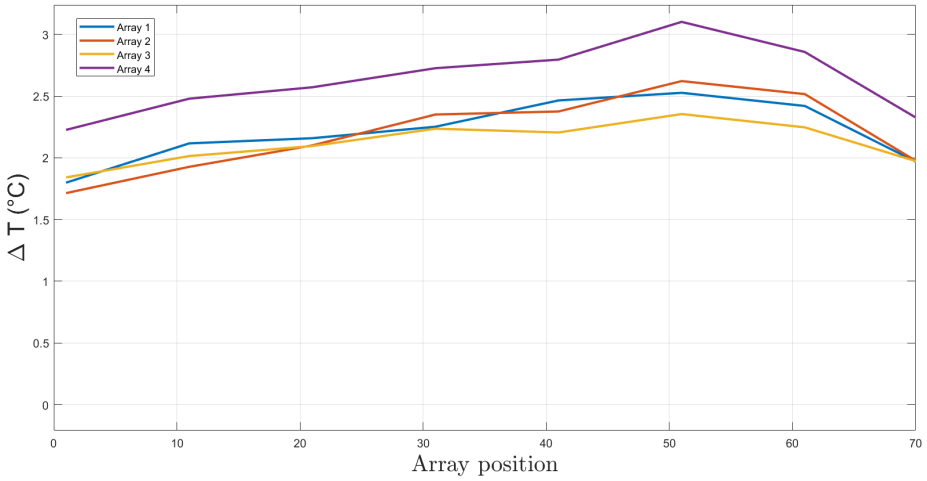


**Figure 7.12:** Temperature profile of a diffuser inserted in the agar block without gold nanoparticles. The test is conduced with 4A current source for 60s.

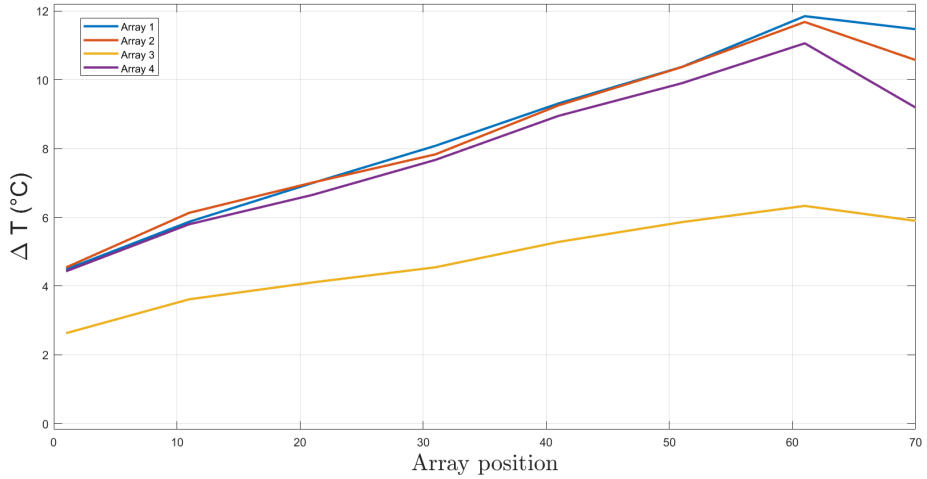


**Figure 7.13:** Temperature profile of a diffuser inserted in the agar block with gold nanoparticles, concentration 10%. The test is conduced with 4A current source for 60s.

# Chapter 8

# Conclusions

The Master's Thesis project focused on the creation of fiber-based delivery devices for medical applications in cancer treatments. In particular, the fabrication of a uniform diffuser through a suitable femto-second laser inscription has been performed, trying to obtain a final device with good uniformity in the light irradiaiton toward the outside of the fiber. The uniformity is a fundamental requirements for the application of said devices to the photodynamic therapy, which aims at treating cancer using the photochemical reaction generated by a particular chemical substance, the photosensitizer, upon infrared irradiation. The result of the medical procedure is a non-invasive treatment thanks to the small dimensions of the optical fibers that do no need any surgical procedure to be inserted in the human body. The uniformity of the diffuser is of primary importance when devising a reproducible and predictable treatment, since the irradiation of the tumor should uniformly affect the tumoral mass, avoiding the overexposure of the healthy tissues or the underexposure of the region under treatment.
The design of the diffuser faced the difficulty of writing a uniformly diffusing device without resorting to any rotating stage, absent in the femto-second laser machine used for the fabrication. Moreover, it was also needed to come up with a suitable experimental set-up for the characterization of the diffusers, that finally relied on the light-to-thermal conversion capacity of the agar gel. Theoretically designing the diffusers and the inscription to be made is a very complicated task due to the difficulty of simulating the interaction between the electromagnetic field and the perturbation introduces by the damages inscribed in the fiber. Given this, the design of the diffuser has been done by experimentally modifying the parameters used for the inscribing the fibers, studying how the different available parameters could modify the light emission from the fiber. The results obtained show that a diffuser inscribed with a

non-uniform power-varying profile produce the best results in terms of longitudinal uniformity, close to the device taken as reference. On the other side, the uniformity characterization and the emission efficiency evaluation are still far from the ideal, given that a more complicated structure should be studied to achieve a result closer to the state of the art. Moreover, it would be of great interest to compare the designed diffusers with a commercially available device, studying their response when applied in analogous experiments.

# Bibliography


[1] Giribabu L. Chilakamarthi U. «Photodynamic Therapy: Past, Present and Future». In: *Chem Rec.* 17(8) (Aug. 2017), pp. 775–802 (cit. on pp. 18, 20).

[2] P. Agostinis et al. «PHOTODYNAMIC THERAPY OF CANCER: AN UPDATE». In: *CA Cancer J Clin* 61(4) (Aug. 2011), pp. 250–281 (cit. on pp. 18, 21).

[3] Patterson MS Wilson BC. «The physics, biophysics and technology of photodynamic therapy». In: *Phys Med Biol* 53(9) (May 2008), R61–109 (cit. on p. 19).

[4] van Lier JE. Sharman WM Allen CM. «Photodynamic therapeutics: basic principles and clinical applications». In: *Drug Discov Today* 4(11) (Nov. 1999), pp. 507–517 (cit. on p. 20).

[5] Paszko E et al. «Nanodrug applications in photodynamic therapy». In: *Photodiagnosis Photodyn Ther* 8(1) (Mar. 2011), pp. 14–29 (cit. on p. 22).

[6] D.Y. Kim H.S.; Lee. «Near-Infrared-Responsive Cancer Photothermal and Photodynamic Therapy Using Gold Nanoparticles.» In: *Polymers* 961 (Oct. 2018) (cit. on p. 23).

[7] Michele M. Kim and Arash Darafsheh. «Light Sources and Dosimetry Techniques for Photodynamic Therapy». In: *Photochemistry and Photobiology* 96 (2020), pp. 280–294 (cit. on p. 27).

[8] van Swol CF. Verdaasdonk RM. «Laser light delivery systems for medical applications.» In: *Phys Med Biol.* 42(5) (May 1997), pp. 869–94 (cit. on p. 30).

[9] van den Bergh HE. Mizeret JC. «Cylindrical fiberoptic light diffuser for medical applications.» In: *Lasers Surg Med.* 19(2) (1996), pp. 159–67 (cit. on p. 31).

[10] Darafsheh A. Kim MM. «Light Sources and Dosimetry Techniques for Photodynamic Therapy.» In: *Photochem Photobiol.* 96(2) (Mar. 2020), pp. 280–294 (cit. on p. 31).

[11] Ströbl S et al. «Homogeneously Emitting, Mechanically Stable, and Efficient fs-Laser-Machined Fiber Diffusers for Medical Applications.» In: *Lasers Surg Med.* 54(4) (Apr. 2022), pp. 588–599 (cit. on pp. 32, 34).

[12] Manfred Fischer Ivan S. Melnik Raimund Hibst and Gabriela Flemming. «New modified optical fiber tips for medical applications.» In: *Opt. Eng.* 32(2) (Feb. 1993) (cit. on p. 34).

[13] Duncan Bell Rebecca L Kozodoy Scott L. Lundahl and James A. Harrington. «Three-dimensional characterization of the light distribution from diffusing cylindrical optical-fiber tips.» In: *Appl. Opt.* 33 (1994), pp. 6674–6682 (cit. on p. 34).

[14] Y. Liu, W. Chen, Hao Yu, Riccardo Gassino, Andrea Braglia, Massimo Olivero, Guido Perrone, and Alberto Vallan. «All-fiber probe for laser-induced thermotherapy with integrated temperature measurement capabilities». In: *Progress in Biomedical Optics and Imaging - Proceedings of SPIE* 9317 (Mar. 2015). DOI: 10.1117/12.2078760 (cit. on p. 37).

[15] Perrone G Barbero F Gul S and Fenoglio I. «Photoresponsive Inorganic Nanomaterials in Oncology.» In: *Technology in Cancer Research & Treatment.* 22 (2023), pp. 1–19 (cit. on p. 55).